MINOR RESEARCH PROJECT

Project title

"GROWTH AND CHARACTERIZATION OF MIXED CRYSTALS OF TGS-ADP AND TGS-KDP"

MRP(S)-0569/13-14/KATU008/UGC-SWRO

Final report
Submitted To

The Joint secretary and Head
South Western Regional Office (SWRO)

University grants commission
P.K. Block, Gandhinagar, Palace Road
Bangalore – 560 009

Submitted by

Roopa.V, M Sc., M.Phil
Principal Investigator, Department of Physics

Sree Siddaganga College of Arts, Science and Commerce for Women, Tumkur
Affiliated to Tumkur University
Reaccredited by **NAAC** with **'A'** Grade
B.H.Road, Tumkur – 572 102 Phone: 0816-2272312, Fax: 0816-2272312
Web : www.sscwtumkur.org

DECLARATION AND CERTIFICATE

I hereby declare and certify that, the Minor Research Project entitled **"Growth and Characterization of mixed crystals of TGS-ADP and TGS-KDP"** MRP(S)-0569/13-14/KATU008/UGC-SWRO dated 28-Mar-14 is a bonafide record of research work carried out by me during the year 2014-2016. Further certify that the work presented in the report is original and carried out according to the plan in the proposal and guidelines of the University Grants Commission.

Roopa V
Principal Investigator

ACKNOWLEDGEMENT

I would like to thank University Grants Commission (UGC) for providing financial assistance under Minor Research Project MRP(S)-0569/13-14/KATU008/UGC-SWRO to carry out this research work on **"Growth and Characterization of mixed crystals of TGS-ADP and TGS-KDP".**

I would like to thank Dr.Praveen Kumar, IISC, Bangalore for UV-Visible measurement. I would also like to thank Prof.P.K.Das, IISC, Bangalore for SHG measurement.

It is a great privilege to put on record my profound sense of gratitude to Dr.R.Ananda Kumari, Associate Professor in Physics, Sree Siddaganga College of Arts, Science and Commerce, Tumkur, for her invaluable guidance, constant encouragement and suggestions given during the course of this work.

I am thankful to our Principal Prof.V.Nalinakshi, Sree Siddaganga College for Women, Tumkur, for her co-operation during the course of this work.

I am grateful to my family, who are supportive and given inspiration in all walks of my life.

CONTENTS

CHAPTER 1

INTRODUCTION

1.1 CRYSTALS

Crystal growth is a vital and fundamental part of material science and engineering, because crystals of suitable size and perfection are required for fundamental data acquisition and for practical devices such as detectors, integrated circuits and for other millions and millions of applications [1]. Behind every new solid state device there stands a single crystal. The ever increasing application of semiconductor based electronics creates an enormous demand for high quality semiconducting, ferroelectric, piezoelectric, oxide single crystals.

Ferroelectric materials pervaded a broad range of industrial and domestic applications as a result of their large electro-optic and nonlinear optical coefficients, and are of fundamental interest due to their polarization hysteresis, photo refraction, piezoelectricity, and pyro electric properties. This range of electrical and optical phenomena has been exploited in a number of technological applications which include electro-optic scanners and lenses, integrated optics, piezoelectric transducers, pyro electric detectors, ferroelectric memories, surface acoustic wave devices and quasi – phase matched crystals for nonlinear frequency conversion.

Ferroelectric crystals are phase-transforming materials. There exists a critical temperature, called the Curie temperature, such that above this temperature they are paraelectric with non-polar structures. However, on cooling below the Curie point, the unit cell is spontaneously polarized with a spontaneous lattice distortion. The crystals are both piezoelectric and ferroelectric where the piezoelectric behavior exhibits along the spontaneous polarization direction. Another feature of this transformation is that there is a reduction in crystallographic symmetry, and this creates more than one symmetry-related polarized state. Each of them is equally favorable in the absence of external field and load. These preferred states, which are characterized by pairs of spontaneous strain and polarization, are commonly called the ferroelectric variants. Very often, a mixture of variants rather than a single variant coexists in these materials; and multiple domains, each of which is a region of uniform spontaneous strain and polarization, are observed with scales ranging from few to hundreds of nanometers. Adjacent domains are separated by a domain wall

which has a well-defined crystallographic orientation. As a result, domains form highly intricate and characteristic patterns in ferroelectric materials[2].

1.2 NUCLEATION

Nucleation is an important phenomenon in crystal growth and is the pre- cursor of crystal growth and of the overall crystallization process. The condition of super saturation alone is not sufficient cause for a system to begin crystallization. Before crystals can grow, there must exist in the solution a number of minute solid bodies known as centers of crystallization, seeds, embryos or (nuclei). The formation of stable nuclei occurs only by the addition of a number of molecules (A1) until a critical cluster is formed. In general,

$$A(n-1) + A1 = An \text{ (critical)}$$

Any further addition to the critical nucleus results in nucleation followed by growth. Once these nuclei grow beyond a certain critical size, they become stable under the average condition of super saturation of the solution. Further, the creation of a new phase in the homogeneous solution demand the expenditure of certain quantity of energy.

The total Gibbs free energy change, ΔG of the embryo between the two phases associated with this process is then given as Δ?=Δ? ?+Δ? ?
where ΔGS is the surface free energy and ΔGv is the volume free energy. For a spherical nucleus of radius r, Δ?=4? ?2 ?+43? ?3Δ? ?
where γ is the interfacial tension and ΔGv is the free energy change per unit volume and is a negative quantity.

Nucleation may occur spontaneously or it may be induced artificially and they are usually referred to as homogeneous and heterogeneous nucleation respectively. As shown in Figure 1.1, the term primary is used for both homogeneous and heterogeneous nucleation even in systems that do not contain crystalline matter. On the other hand, during secondary nucleation, nuclei are often generated in the vicinity of the crystals present in the supersaturated system. This process involves the dislodgement of the nuclei from the parent crystal at super saturation in which primary homogeneous nucleation cannot occur. When a supersaturated solution is disturbed by agitation, friction or mechanical stimulus in the presence of the crystalline substance of the solute, embryos are formed at the surfaces of the parent crystal. These embryos give rise to secondary nucleation.

If the nuclei form homogeneously in the interior of the phase, it is called homogeneous nucleation. If the nuclei form heterogeneously around ions, impurity molecules or on dust particles, on surfaces or at structural singularities such as imperfections or dislocations, it is known as heterogeneous nucleation [3].

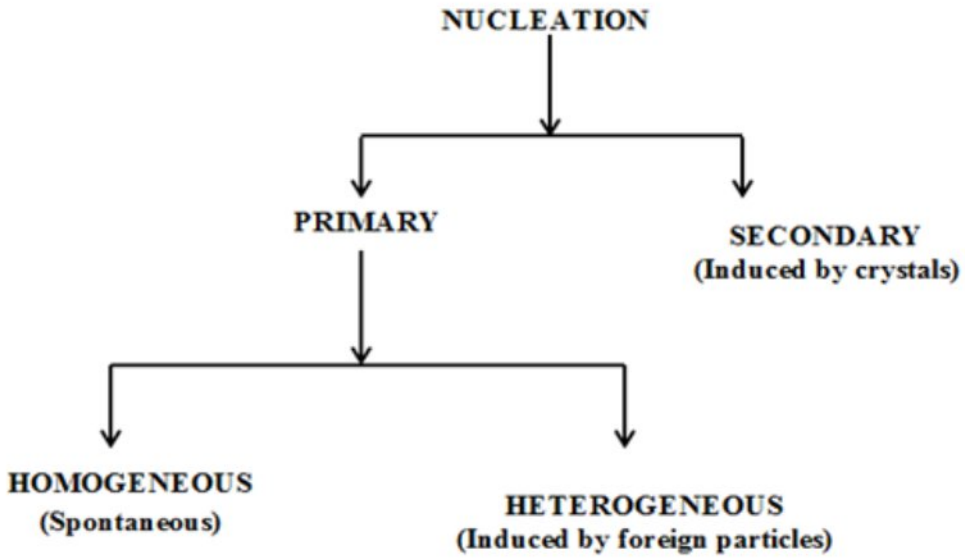

Figure 1.1 Classification of nucleation

In general, the crystallization process takes place by three steps:

1. Achievement of super saturation or super cooling

2. Formation of crystal nuclei and

3. Growth of crystal.

All the above steps may occur simultaneously at different regions of a crystallization unit. However an ideal crystallization process consists of a strictly controlled stepwise program.

1.2.1 EXPRESSION OF SUPER SATURATION

The super saturation of a system may be expressed in a number of ways. The basic units of concentration as well as temperature must be specified. The concentration driving force (ΔC), the super saturation ratio (S) and relative super saturation (σ) are related to each other as follows:

The concentration driving force $\Delta C = C - C^*$

where C is the actual concentration of the solution at a given temperature and C* is the equilibrium concentration at a given temperature.

Super saturation ratio $S = C / C^*$

Relative super saturation $\sigma = (C - C^*) / C^*$

$\sigma = S - 1$

If the concentration of a solution can be measured at a given temperature and the corresponding equilibrium saturation concentration is known, then, it is easier to calculate the super saturation.

1.3 METHODS OF CRYSTAL GROWTH

Growth of crystal ranges from a small inexpensive technique to a complex sophisticated expensive process and crystallization time ranges from minutes, hours, days and to months. The starting points are the historical works of the inventors of several important crystal growth techniques and their original aim. The methods of growing crystals are very wide and mainly dictated by the characteristics of the material and its size [4].

The methods of growing single crystals may be classified according to their phase transformation as given below.

Solid Growth - Solid-to-Solid phase transformation

Liquid Growth - Liquid to Solid phase transformation

Vapour Growth - Vapour to Solid phase transformation

Based on the phase transformation process, crystal growth techniques are classified as solid growth, vapour growth, melt growth and solution growth [5].The basic common principle in all these methods is that a nucleus is first formed and it grows into a single crystal by organizing and assembling ions or molecules with specific interactions and bonding, so that the process is slow and multiple nucleation's is minimized. Crystal growth process and size of the grown crystal differ widely and are determined by the characteristics of the material. An efficient process is the one, which produces crystals adequate for their use at minimum cost. The growth method is essential because it suggests the possible impurity and other defect concentrations. Choosing the best method to grow a given material depends on material characteristics.

1.3.1 GROWTH FROM SOLUTION

The crystal growth from liquid can be classified into six categories namely,

i) Melt growth
ii) High temperature solution growth (Flux growth)
iii) Hydrothermal growth
iv) Gel growth
v) Electro crystallization and
vi) Low temperature solution growth

There are a number of growth methods in each category. Among various methods of growing single crystals, solution growth at low temperature occupies a prominent place owing to its versatility and simplicity. Growth from solution occurs close to equilibrium conditions and hence crystals of perfection can be grown. Study of anisotropy of the properties of crystals requires specimens cut in different orientations from the same single crystal. This can be easily done from crystals of large size.

1.3.1.1 GROWTH FROM MELT

Melt growth is the process of crystallization by fusion and resolidification of the pure material. In this technique, apart from possible contamination from crucible materials and surrounding atmosphere, no impurities are introduced in the growth process and the rate of growth is normally much higher than that possible by other methods. Mainly, for the latter reason, melt growth is commercially the most important method of crystal growth. The preferential role of the electrochemical process responsible for the change in composition of the crystals when they grow in melt in an applied field has been studied [6].

The growth from melt can further be sub-grouped into various techniques listed below.
i) Bridgman technique
ii) Czochralski technique
iii) Zone melting technique
iv) Verneuil technique
v) Heat exchanger method
vi) Skull melting and
vii) Shaped crystal growth

The major practical factors to be considered during growth of crystals from melt are:
(a) Volatility, (b) The chemical reactivity and (c) The melting point.

1.3.1.2 HIGH TEMPERATURE GROWTH (FLUX GROWTH)

Flux and hydrothermal growths form the category of high temperature solution growth. In the growth of crystals from high - temperature solutions, the constituents of the material to be crystallized are dissolved in a suitable solvent and crystallization occurs as the solution becomes critically supersaturated. The super saturation may be promoted by evaporation of the solvent, by cooling the solution or by a transport process in which the solute is made to flow from a hotter to a cooler region. The high temperature crystal growth can be divided into two major categories: first one is growth from single component systems and the second one is that from multi-components. In this method, a solid (molten salt / flux) is used as the solvent instead of liquid and the growth takes place well below the melting point of the solute. The success of crystal growth from high temperature solution largely depends on the selection of the solvent system.

This technique can be used for the crystallization of oxide compounds which generally have high melting points as well as for materials which have phase transitions below the melting point [7]. The crystals grown from melt have lower concentration of equilibrium defects and lower dislocation density. One major disadvantage of this method is the corrosive nature of the fluxes used, which attack the common furnace materials.

1.3.1.3 HYDROTHERMAL GROWTH

The term hydrothermal means, literally, “hot water”. Hydrothermal also implies conditions of high pressure as well as high temperature. Closely related to growth from aqueous solution at ambient or near-ambient conditions is the growth from hydrothermal solution. Hydrothermal growth is usually defined as the use of an aqueous solvent at elevated temperature and pressure to dissolve a solute which would be virtually insoluble at ambient conditions. The disadvantages of the hydrothermal techniques are mainly associated with high pressure and inability to observe growth during the process. Quartz is the crystal grown industrially by this technique [8].

1.3.1.4 GEL GROWTH

The growth of variety of crystals having immense importance for their practical consideration and theoretical interest has been achieved by gel technique. The importance of the gel growth is attributed to its simplicity in technique, effectiveness in growing single crystals of compounds that cannot easily be grown by other methods. Though the origin of the method dates back to 1899 – the famous work of Liesegang who discovered the periodic crystallization in gels, interest in gel technique received attention only after the work of Henisch and his co-workers [9]. Crystal growth in gels is a promising technique for growing single crystals of substances which are slightly soluble in water and which cannot be grown conveniently from melt or vapour. The gel method has also been applied to study the crystal formation in urinary calculi and rheumatic diseases.

1.3.1.5 ELECTROCRYSTALLIZATION

Electro crystallization is the basis for important fields such as corrosion, energy storage and generation, electro deposition, electronics material development, electro refining, electro twinning etc. Crystallization without chemical transformation or charge transfer is the simplest case. In certain instances, the crystallization is determined by a chemical transformation occurring prior to or simultaneously with the crystallization process. The role played by the chemical reaction is to supply the material, which crystallizes. Electro crystallization is the process, which leads to the formation of a new face at the electrode/electrolyte interface, which in turn plays a major role.

1.3.1.6 LOW TEMPERATURE SOLUTION GROWTH

The method of crystal growth from low temperature aqueous solution is extremely popular in the production of many technologically important crystals. It is the most widely used method for the growth of single crystals, when the starting materials are unstable at high temperatures and also which undergo phase transformations below melting point [10]. The growth of crystals by low temperature solution growth method involves weeks, months and sometimes years. Much attention has been paid to understand the growth mechanism of the process. Though the technology of growth of crystals from solution has been well perfected, it involves meticulous work and much patience.

Materials having moderate to high solubility in temperature range, ambient to 100^{o}C at atmospheric pressure can be grown by low temperature solution growth method. The

mechanism of crystallization from solutions is governed, in addition to other factors, by the interaction of ions or molecules of the solute and the solvent. This is based on the solubility of substance on the thermo dynamical parameters of the process; temperature, pressure and solvent concentration. This method is the most widely used method for the growth of single crystals, when the starting materials are unstable at high temperature. This method is widely used to grow bulk crystals, which have high solubility and have variation in solubility with temperature. The advantages of crystal growth from low temperature solution nearer the ambient temperature results in the simple and straight forward equipment design which gives a good degree of control of accuracy of ±0.01ºC. In the low temperature solution growth, crystals can be grown from solution, if the solution is supersaturated i.e., it contains more solute than it can be in equilibrium with the solid. Due to the precise temperature control, super saturation can be very accurately achieved. Also efficient stirring of solution reduces fluctuations to a minimum.

The three principal methods used to produce required super saturation are:

i. Slow cooling of the solution

ii. Slow evaporation of the solvent

iii. The temperature gradient method.

Low temperature solution growth is a well-established technique due to its versatility and simplicity. It is possible to grow large crystals of high perfections as the growth occurs close to equilibrium conditions [12]. It also permits the preparation of different morphologies of the same materials by varying the growth conditions[13].

1.3.1.6.1 SLOW COOLING METHOD

This is the most suitable method among various methods of solution growth. However, the main disadvantage of slow cooling method is the need to use a range of temperatures. The possible range of temperature is usually narrow and hence much of the solute remains in the solution at the end of the growth run. To compensate this effect, large volume of solution is required. The use of wide range of temperatures may not be desirable because the properties of the grown crystals may vary with temperature. Temperature stability may be increased by keeping the solution in large water bath or by using a vacuum jacket. Achieving the desired rate of cooling is a major technological hurdle. This technique needs only a vessel for the solution in which the crystals grow. The height, radius and volume

of the vessel are so chosen as to achieve the required thermal stability. Even though this method has technical difficulty of requiring a programmable temperature controller, it is widely used with great success. In general, the crystals produced are small and the shapes of the crystals are unpredictable.

1.3.1.6.2 SLOW EVAPORATION METHOD

As far as the apparatus is concerned, slow cooling and slow evaporation methods are similar to each other. In this method, the saturated solution is kept at a particular temperature and provision is made for evaporation. If the solvent is non-toxic like water, it is permissible to allow evaporation into the atmosphere. Typical growth conditions involve a temperature stabilization of about 0.05ºC and rate of evaporation of a few mm3/h. The evaporation technique has an advantage viz. the crystals grow at a fixed temperature. But, inadequacies of the temperature control system still have a major effect on the growth rate. This method can effectively be used for materials having very low temperature coefficient of solubility. But the crystals tend to be less pure than the crystals produced by slow cooling technique because, as the size of the crystal increases, more impurities find place in the crystal faces. Evaporation of solvent from the surface of the solution produces high local super saturation and formation of unwanted nuclei. Small crystals are also formed on the walls of the vessel near the surface of the liquid from the material left after evaporation. These tiny crystals fall into the solution and hinder the growth of the crystal. Another disadvantage lies in controlling the rate of evaporation. A variable rate of evaporation may affect the quality of the crystal. In spite of all these disadvantages, this is a simple and convenient method for growing single crystals of large size.

One can grow crystal at a fixed temperature by simplifying the temperature-control system and in practice make it more efficient. Also, this makes it more reliable. All these can be satisfied by letting the solvent evaporate. If we have a solution of volume V containing a weight concentration C, then $C\,(dV/dt) = \rho(At\ f) - V(dC/dt)$ where f is the growth rate on a face of area Atand (At f) is the sum of the products for all the faces. For stable growth we need to ensure the stability of growth rate(Brice, J.C., 1986). Excellent quality crystals of ferroelectric and piezo-electric materials such as Ammonium dihydrogen phosphate (ADP), Potassium dihydrogen phosphate (KDP) and Triglycine sulphate (TGS) are commercially grown for use in devices by the low temperature solution growth method.

1.4 FERROELECTRICS

Ferroelectrics are materials that display an electric polarization in the absence of an external applied electric field, together with the property that the direction of the polarization may be reversed by an electric field. The study of the properties of ferroelectric materials and the attempt to understand the nature of the ferro electric state constitute the field of ferro electricity. Any macroscopic collection of matter is, to a very high degree of accuracy, electrically neutral, there being very nearly equal numbers of positive and negative charge, however, the positive and negative charges are not necessarily distributed in a homogeneous or symmetric manner. If the "centers of gravity" of the positive and negative charge distributions within a volume of material do not coincide, the material is said to have an electric dipole moment. The net dipole moment per unit volume is defined as the spontaneous polarization [13].

1.4.1 CLASSIFICATION OF FERROELECTRIC MATERIALS

Most of the ferroelectric materials have perovskite structure and many could form solid solutions by addition of dopant material. Ferroelectric can be divided into two main groups, displacive (polarization along several axes that are equivalent in the unpolar state) and order-disorder (polarization along only one axis, “up” or “down”) [14].

Displacive ferroelectric materials exhibit the polarization due to ionic displacements of certain atoms in the crystal lattice dynamics. The displacive class crystal contains oxygen octahedra, so it is also named as oxygen octahedral ferroelectrics. The most typical displacive ferroelectrics is perovskite type, for example $BaTiO_3$, $KNbO_3$, $PbTiO_3$, etc [15]. The generic formula of perovskite type is ABO_3 where “A” represents a monovalent or divalent metal (Ba, Pb, Sr, Ca, Bi, K or Na) and “ B ” represents tetravalent or pentavalent (Ti, Nb, Zr, Ta, Mo, W and Fe), possible combinations are $A^{2+}B^{4+}$ or $A^{1+}B^{5+}$.

The order-disorder class of ferroelectrics includes crystals in which the spontaneous polarization is a result from the linear ordering of the proton ions in the structure. There are two major groups of order-disorder ferroelectrics. The first one consists of elements, such as phosphates, sulphates, fluoroberyllates, cyanides, periodates and glycine compounds, where the spontaneous polarizations appears as a result of the ordering of protons in the hydrogen bonds. They are known as hydrogenbonded ferroelectrics. The second group consists of tartrates, potassium nitrate, sodium nitrate, dicalcium strontium propionate and

tetramethylammomium chloro- and bromomercurates. In this group, spontaneous polarization is caused by the arbitrary ordering of radicals, which takes place from hindered rotation. The typical examples of order-disorder ferroelectrics are sodium nitrite ($NaNO_2$), potassium dihydrogen phosphate (KDP) and triglycine sulphate (TGS).

1.4.2 GENERAL PROPERTIES OF FERROELECTRICS

1.4.2.1 POLARIZATION

Polarization (P) is the electric dipole moment per unit volume, and is related to dielectric displacement D through the linear expression ?=?+?0?.

where ?0, the as the permittivity of free space is 8.854×10^{-12} Coulomb/volt. In ferroelectric materials both D and P are non-linear functions of E and can depend on the previous history of the material. When the term ε0E in the above expression is negligible compared to P (as in the case of most ferroelectric materials), D is nearly equal to P. The polarizability of a material is the measure of the extent to which electric dipoles are formed by the atoms and molecules by the application of electric field. The dipoles may arise due to a variety of mechanisms, any or all of which will contribute to the value of polarization. They are electronic polarization, ionic (Atomic) polarization, orientation polarization and space-charge polarization.

In electronic polarizability there is a displacement of the electronic cloud with respect to the nucleus. As the dipole moment is defined as the product of the charge and the shift distance, it is also proportional to the field strength. Atomic or ionic polarizability is due to separation of positive and negative ions in the crystal. It should be distinguished from electronic polarization, where the electron cloud of an atom shifts with reference to its own nucleus. Some molecules carry a dipole moment even in the absence of electric field. When an electric field is applied on such molecules, they tend to align themselves in the direction of applied field. The polarization due to this alignment is called orientation polarization. Space charge polarization occurs due to the accumulation of charges at the interfaces in multiphase materials. The ions diffuse over appreciable distances in response to the applied field, giving rise to a redistribution of charges in the dielectric medium. Hence the total polarizability of the material is the sum of all these polarizations.

1.4.2.2 SPONTANEOUS POLARIZATION

Spontaneous polarization (PS) is defined as the magnitude of polarization within a single ferroelectric domain in the absence of an external electric field. Spontaneous polarization is a fundamental property of all pyroelectric crystals, but it is reversible and reorientationable in ferroelectrics only. Most ferroelectric phase originates from a non-polar prototypic phase and all of the polarization is reorientationable. However, if the prototypic phase is polar, only a proportion of the total spontaneous polarization may be reoriented, the reorientationable or reversible process is commonly called as the spontaneous polarization. The magnitude of Ps in a single crystal is directly related to the atomic displacements that occur in ferroelectric reversal and may be calculated from the atomic positions within the unit cell if known. Designating Δi as the component of the atomic displacement vectors joining the ith atom positions in the original and reversed orientations along the direction of PS, Zi the effective charge on the ith ion and V as the unit cell volume, then $PS=(1/2V)\Delta iZi$. The spontaneous polarization of single domain materials usually laid within the range 10^{-7}and10^{-4} Coulomb/cm^{-2}[16].The spontaneous polarization can be calculated directly from charge density obtainable by X-ray diffraction structural measurements, corrected for the charge transferred across unit cell boundaries.

1.4.2.3 FERROELECTRIC DOMAIN

A ferroelectric crystal consists of regions of homogeneous polarization that differ only in the direction of polarization. These regions are called ferroelectric domains. When temperature decreases and becomes lower than the Curie temperature, in the absence of external electrical field and mechanical stress, many small regions known as domains will form inside the crystal. Ferroelectric domain is the region within each of which the polarization align in the equal orientation but in adjacent domains, the polarizations is in different directions .The sum of all different oriented dipoles in all domains gives the resultant polarization. A single crystal that contains no domains is considered as in a single-domain or mono-domain state. The single-domain state in single crystal of ferroelectric materials can be achieved by poling (polarization reversal in strong electric field) shown in figure 1.2.

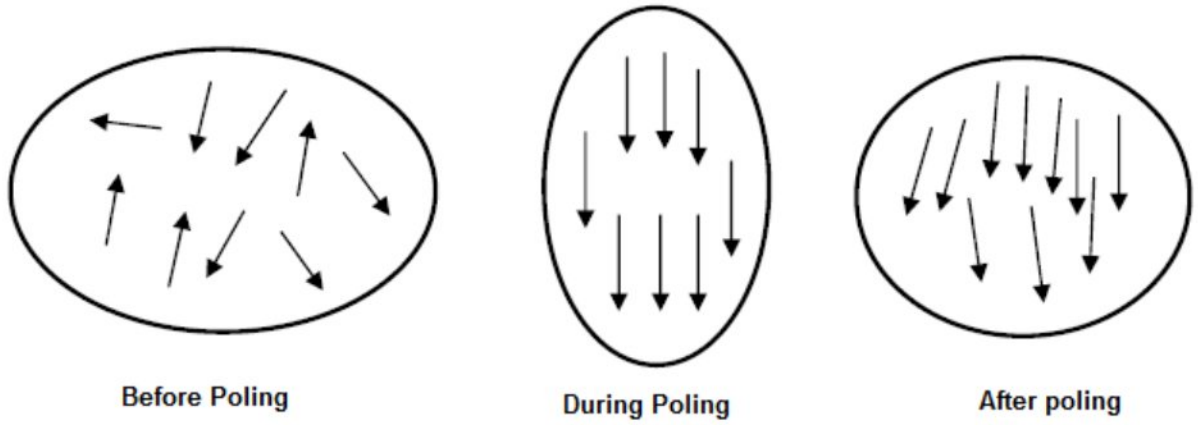

Figure 1.2 Effect of poling on dipole orientation [17]

The region between two adjacent domains is called domain wall. Within this wall, the spontaneous polarization changes its direction. The wall between anti parallel domains is probably only a few lattices spacing thick, whereas the wall between domains polarized at right angle to each other is probably thicker [18].

At transition temperature, the spontaneous polarization forms surface charges and stray charges accumulate on the surface of ferroelectric material. When there is non-homogeneous distribution of the spontaneous polarization, the surface charge produces an electric field, denoted as depolarization field Ed which is in the opposite direction to the spontaneous polarization. Depolarization field will disturb the stability of single domain state ferroelectrics [19]. When the ferroelectric splits into domains with opposite directions and minimize the electrostatic energy associated with the depolarization field. This means the reduction of the energy of the depolarization field formed upon cooling through the ferroelectric phase transition point. Similar to ferromagnetic, the splitting of a ferroelectric crystal into many domains minimizes the energy and stabilizes the whole system.

The types of domain wall in a ferroelectric crystal depend on the symmetry of both non-ferroelectric and ferroelectric phases of the crystal [20]. The polarizations in adjacent domains always make a definite angle between each other. When a crystal is cooled from the paraelectric phase to ferroelectric phase, at least two equivalent directions along the spontaneous polarization may occur. A system with two possible orientations of polarization, such as triglycine sulphate, KH2 PO4 and Rochelle salt has anti-parallel domains. For systems with more than two possible orientations of the dipoles, a more complicated domain

structure may occur. For example, BaTiO3 in the tetragonal phase with six possible directions of polarization can contain both 180º and 90º domains and the corresponding walls. However in the monoclinic and rhombohedral phases, 60º walls occur in addition to 90º and 180º walls [21]. Simple diagrams of 180º and 90º domains and the corresponding domain walls are shown in figure. 1.3.

Figure 1.3 A simple sketch of domain walls: (a) 180º (b)90º

Domains also give contribution in polarization switching in ferroelectric crystal. An applied electric field can then switch these domains from one orientation state to another, just as in ferromagnetics. The switching from one domain orientation to another involves work performed on the material, and so the free energy must change from one state to the other [22]. The reversible polarization is accompanied either by domain wall motion (the growth of existing domains anti-parallel to the applied field) or by the nucleation and growth of new anti-parallel domains.

1.4.2.4 FERROELECTRIC HYSTERESIS

Using the domain concept, the occurrence of hysteresis in the polarization 'P' versus field 'E' relationship can be explained as follows. Considering a crystal, which initially has an overall polarization equal to zero, i.e., the sum of the vectors representing the dipole moments of the individual domain vanishes. When an electric field is applied to the crystal, the domains with polarization components along the applied field direction grow at the expense of the "antiparallel" domains; thus the polarization increases. When all domains are aligned in the direction of the applied field the polarization saturates and the crystal becomes a single domain. A further increase in the polarization with increasing applied field results from "normal polarization" effects; rotation of domain vectors may also be involved if the external field does not coincide with one of the possible directions of spontaneous polarization. The extrapolation of the linear part AB (saturation value of polarization) to zero external field as shown in figure. 1.4, gives the spontaneous polarization Ps (since in the relation between electric displacement, field and polarization ?=?+?0?). In the above relation the polarization arises from both the polarization of the material in the presence of a field PE = χE and from

the spontaneous alignment of dipoles in the ferroelectric Ps. The spontaneous polarization and its dependence on temperature or on other external conditions that might be imposed can be measured by displaying the hysteresis loop on an oscilloscope screen. When the applied field for a crystal corresponding to point B in figure 1.5 is reduced; the polarization of the crystal decreases, but for zero applied fields there remains the remanent polarization (Pr) where Pr refers to the crystal as a whole.

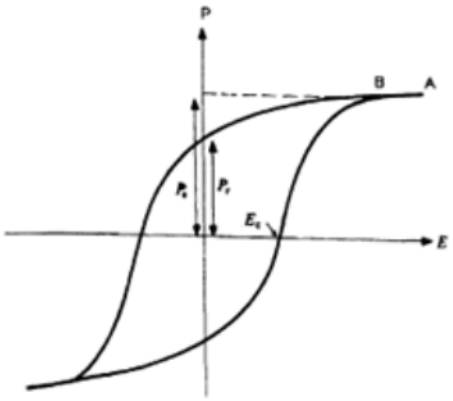

Figure 1.4 A Hysteresis loop illustrating the coercive field EC, spontaneous polarization PS and the remanent polarization Pr.

In order to remove the remanent polarization (P,), the polarization of the crystal must be reversed and this occurs only when a field in the opposite direction is applied. The field required to make the polarization zero is called the coercive field Ec [23].

1.4.2.5 PHASE TRANSITION

Another important characteristic of ferroelectric is structural phase transition from the paraelectric phase into the ferroelectric phase. The phase transition of ferroelectric is generally a structural phase transition where the spontaneous polarization appears as the order parameter below the transition temperature. Commonly, ferroelectric materials undergo a structural phase transition from random paraelectric phase at high temperature into ordered ferroelectric phase at low temperature. When the temperature decreases, the spontaneous polarization will vanish at a characteristic temperature, named as Curie point or Curie temperature C T at which the phase transition takes place. When temperature is higher than the Curie temperature T > TC, the material is in the para electric phase and the polarization equals to zero. When temperature is lower than the Curie temperature TC< T, the material is in the ferroelectric phase with a non-zero polarization. When the temperature is in the vicinity

of the Curie point, the ferroelectric materials show anomalies in the dielectric, elastic, thermal and other thermodynamic properties [24].

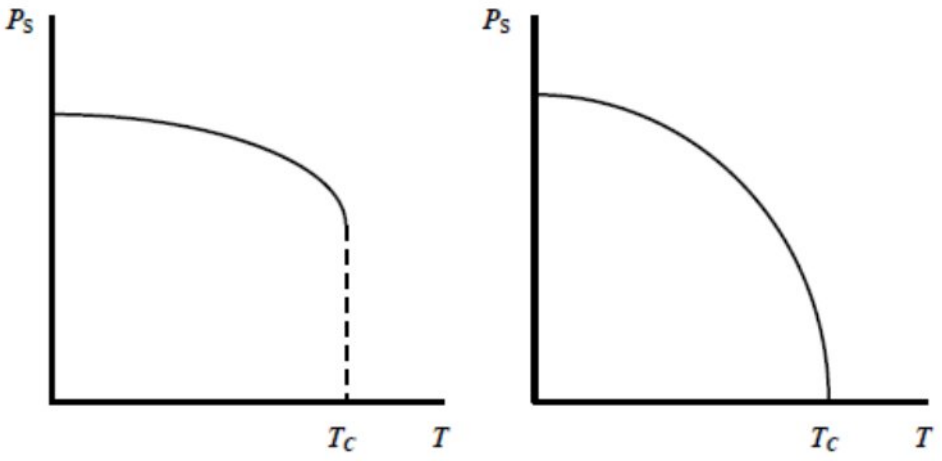

Figure 1.5 Ferroelectric phase transitions in the vicinity of the Curie temperature TC .The temperature dependence of PS: (a) first-order transition and (b) second- order transition (Blinc, R. and Zeks, B., 1974).

1.4.2.6 DIELECTRIC SUSCEPTIBILITY

The gradient of the hysteresis loop connecting E and P equals to the electric susceptibility. The susceptibility of a material describes the variation of polarization which response to the changes in the applied field

In ferroelectric material, the value of dielectric constant or susceptibility varies with the changes of temperature. The temperature dependence of dielectric constant ε (T) is shown in figure. 1.6. The transition from ferroelectric phase to paraelectric phase is accompanied by dielectric constant anomaly.

The primary feature of a ferroelectric is the anomalous dependence of its dielectric constant on temperature. The dielectric constant-temperature diagrams for a ferroelectric has one or more very sharp maxima where ε can reach values of several thousands. The temperature at which maxima occur is called Curie temperature. Above the Curie temperature E obeys the Curie Weiss law.

? = ? ?−? + ?0,

where C is a constant and θ is a characteristic temperature which is usually some degrees smaller than the transition temperature Tc, ε0, is a constant contributed by the electronic

polarization. In the vicinity of the transition temperature, ε0 may be neglected since it is of the order of unity and ε >> ε0.

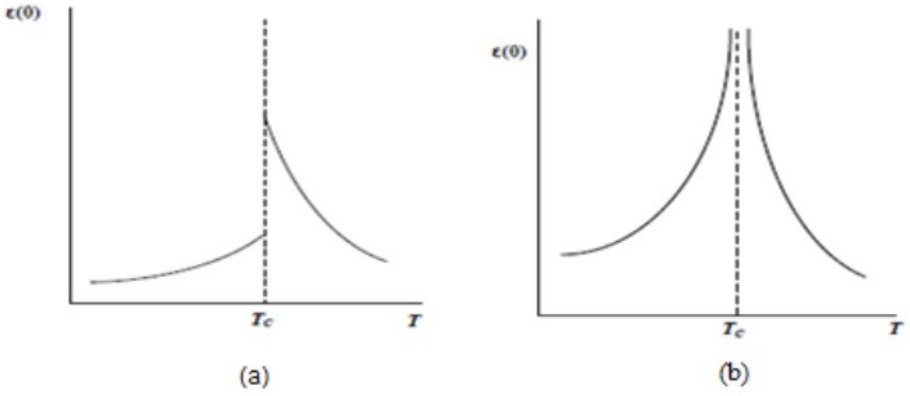

Figure 1.6 Temperature dependence of ε (T) a) first order transition and b) second order transition.

1.4.2.7 PIEZOELECTRIC EFFECTS AND CONSTITUTIVE LAWS

Piezoelectricity is a special property of a group of ferroelectrics. The piezoelectric effect manifests as a spontaneous potential difference across the opposite faces of a volume of material when it is under applied stress. The term "piezo" is from Greek and it means "to press". Therefore, the word "piezoelectric" represents the property of generating electricity by pressing. It was defined by W. Hankel in 1881 as "electric polarization produced by mechanical strain in crystals belonging to certain class, with the polarization being proportional to the strain and changing sign with it". Electric polarization can be reflected by surface charge. Piezoelectricity is attributed to the lack of a center of symmetry of the crystallographic unit cell [25]. Deformation of such a unit cell leads to formation of polarization. Figure 1.7 provides an explanation of why the piezoelectric effect exists. In Figure 1.7 (a), deformation of a unit cell with a center of symmetry does not induce polarization. In Figure 1.7 b, relative displacements of the ions under stress leads to a net polarization.

Piezoelectricity is the ability of certain crystalline materials to develop an electrical charge proportional to an applied mechanical stress. This is also called the direct piezoelectric effect. Piezoelectric materials also show a converse effect, where a geometric strain (deformation) is produced on the application of a voltage.

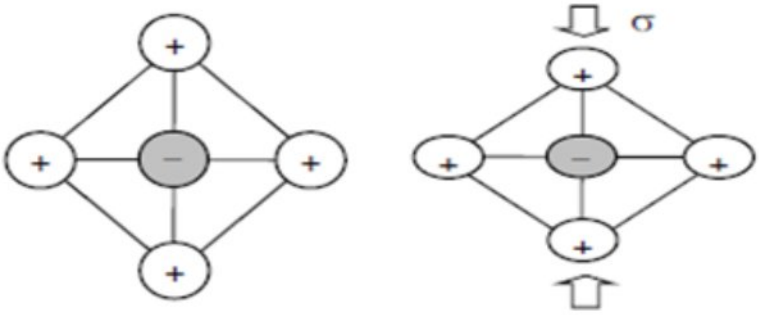

1.7 (a) No piezoelectric effect with a centrosymmetric unit cell

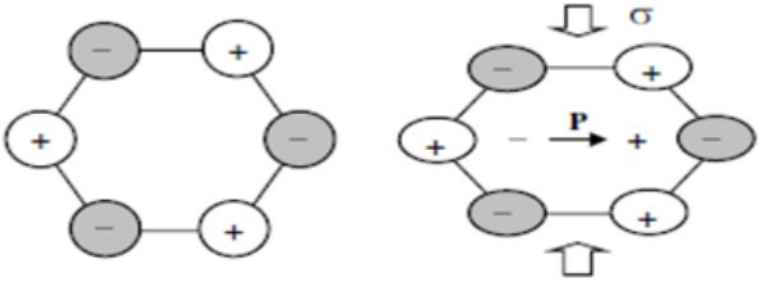

1.7 (b) Piezoelectric effect due to the lack of center of symmetry.

Figure 1.8 Origin of piezoelectricity.

The constitutive equations that describe these two piezoelectric effects are given below:

? ?? = ? ??? ?? ? ? ? + ? ? ??? ?

? ? = ? ?? ?? ? ? + ??? ? ? ?

where D is the dielectric displacement, T is the stress, E the electric field, S the strain, d the piezoelectric coefficient, and the material compliance. The superscripts indicate a quantity held constant: in the case of εT, the stress is held constant, which means that the piezoelectric element is mechanically unconstrained. While in the case sE, the electric field is held constant, which means the electrodes on the element are shorted together.

1.4.3 APPLICATIONS OF FERROELECTRIC MATERIALS

The use of ferro electric materials depends on the switching property, *i.e.,* polarization reversal of ferroelectric materials as well as non-switching uses, which mostly employ the high values of dielectric constant near Tc, Curie temperature. Ferroelectric materials are necessarily also pyroelectric and piezoelectric, the coefficients of which are often

exceptionally large for $T \sim Tc$, so they have additional uses based specifically on these properties.

Switched ferroelectrics are employed in matrix addressed memories; shift registers and switches known as trans chargers or trans polarizers. Combined devices based simultaneously on switched ferroelectric and piezoelectric properties include memories, oscillators and filters, while the analogous use of electro optic properties results in light switches, displays and memories. A variety of display devices make use of circuits containing both ferroelectric and electroluminescent components in which light can be stored and emitted in a controlled manner; this is also possible using photoconductor and ferroelectric components, which also permit direct x-ray to light conversion displays. Switched ferroelectric materials involving semiconductor properties lead to field effect devices and adaptive resistors and transistors. TANDEL, the temperature auto stabilizing non-linear dielectric element, is used in miniature thermostats, frequency multipliers and a variety of transducer and nonlinear devices.

The ferroelectrics possess high dielectric constant because of the non switching property and are useful as capacitors. They exhibit a rapid change of resistivity with temperature and are used as thermistors. The linear or quadratic electro optic effect in ferroelectrics is employed in light deflectors, modulators and displays, and the nonlinear optical effect in second harmonic generation, frequency mixing and optical parametric oscillation. The photorefractive effect is also used to provide permanent or optically erasable holographic storage; it is even possible to provide selective erasure in multiple holographic storage.

Ferroelectrics exhibit strong nonlinear optical effects that can be used for laser frequency doubling and optical mixing. Ferroelectric hysteresis is used in non-volatile computer information storage. The direct piezo electric effect is widely used in sensors such as accelerometers, microphones, hydrophones etc.

1.5 APPLICATIONS OF TRI GLYCINE SULPHATE

TGS is important for understanding the physics of the ferroelectric phenomenon as well as for its applications. Despite its complicated chemical and crystallographic form, it is being studied for several years mainly for two reasons: firstly, its excellent pyroelectric properties and high figure of merit make it suitable for use in the low-power detector

applications where high detectivities are required, e.g. in the setup of spectrometers. Secondly, it is one of the very few ferroelectrics known to exhibit a typical second-order, order - disorder type of phase transition, offering a spectrum of possibilities for understanding the basic mechanism of group-subgroup type of phase transitions in crystalline solids.

Triglycine sulphate (TGS) is an important ferroelectric crystal for infrared (IR) detector applications mainly because of its features which allow operation at room temperature. Pyroelectric sensors based on TGS are uniformly sensitive to radiations in wavelength range from ultraviolet to far-infrared and do not require cooling for operation as compared to quantum detectors, where low temperature cooling is required [26]. PIR devices can detect a person moving into or through a detection zone with high reliability. The slightest positive or negative thermal radiation change in contrast to a background, focused by the appropriate optics, triggers the sensor element. There is no interference between neighboring units due to the passive nature of the detection principle. At the heart of every PIR detector is the pyroelectric crystal. Typical detectors use materials, such as triglycine sulphate (TGS) or lithium tantalite. They are ferroelectric crystals, which have a maximum pyroelectric sensitivity at room temperature and therefore do not require the cooling for detection of temperature changes. Both TGS and lithium tantalite exhibit a large spontaneous electrical polarization below their Curie points.

It is advantageous to grow crystals of TGS with a large area in the plane perpendicular to the polar axis i.e. the (0 1 0) face, for practical applications in large-area infrared detectors and laser-energy meters. These are typically discs, between 2.5 and 7.5 cm in diameter. TGS plates of size 30 mm ×30 mm were used in the fabrication of a pyroelectric energy meter for Nd:YAG laser radiation, whereas for VIDICON applications the diameter of slices should be above 3 inch [27].

1.6 REFERENCES

1. **Brice, J. C., (1986)**, "Crystal Growth Process", John Wiley and Sons, New York.
2. **Arlt, G., Sasko, P., (1980),** "Domain configuration and equilibrium size of domains in BaTiO3 ceramics", J. Appl. Phys. Vol.51, pp.4956–4960.
3. **Claude, A., (2006)**, Ph.D. Thesis. Anna University. Chennai. India.
4. **Santhanaraghavan, P. and Ramasamy, P., (2001),** "Crystal Growth Processes and Methods", KRU Publications, India.
5. **Pamplin, B.R. (1979),** „Crystal Growth", Pergamon Press, Oxford.

6. **Balasanyan, R.N., Gabrielyan, V.T., Kokanyan, E.P., and Feldvary, I., (1990),** "Composition and Homogeneity of LiNbO3 Crystal in Connection with Growth Conditions I. Influence of an electric field", Sov. Phys. Crystallogr., Vol.35, pp. 907-910.
7. **Hubner, K.H., (1969)**, "Uber Die Borate 2BaO.5B2O3, Tief-BaO.B2O3, 2BaO.B2O3 and 4BaO.B2O3", Neues Jahrb. Mineral Monatsh, pp. 335-343.
8. **Ballman, A. A. and Laudise, R. A., (1963)**, "The Art and Science of Growing Crystals", Ed.Gilman J. J., John Wiley and sons, New York.
9. **Henisch, H.K., and Garcia-Rutz, J.M., (1986)**, "Crystal Growth in Gels and Liesegang Ring Formation", J. Crystal Growth, Vol.75, pp. 195-202.
10. **Hooper, R.M., Naranes, R.S., Hearole, B.J and Sherwood, J.N. (1980)**, „Crystal Growth Second Edition", (ed.) Pamplin B.R., Pergamon Press, New York.
11. **Chernov, A.A. (1984)**, „Modern Crystallography, III-Crystal Growth", Springer-Verlag, Solid State Series, Berlin, Vol. 36.
12. **Brice, J. C., (1986)**, "Crystal Growth Process", John Wiley and Sons, New York.
13. **Raj,D.,(1995)**, "Solid State Physics", Ammol Publication, New Delhi.
14. **Kanzig, (1957)**, "Ferro electrics and Antiferro electrics", Academic press, New York.
15. **Xu, Y.**, **(1991)**,"Ferroelectric Materials and Their Applications", North-Holland, Amsterdam.
16. **Kittel, C, (2004),** Introduction to Solid State Physics, Wlley Eastern, NewYork.
17. **Damjanovic, (1998), "**Ferro electric, dielectric and piezo electric properties of ferroelectric thin films and ceramics", Rep.Prog.Phys, Vol.61, p. 1267.
18. **Black more, J. S., (1985)**, Solid State Physics, Cambridge University Press, Cambridge.
19. **Shur, M., (1996),** "Handbook series on semiconductor parameters", World Scientific press.
20. **Fousek, J., and Janovec, C., (1969),**"The orientation of Domain walls in twinned ferroelectric crystals. J. Appl. Phys., Vol.40, pp.135-142.
21. **Zhong, F., Jinming Dong, and Xing,D. Y., (1998),**"Scaling of Hysteresis in Pure and Disordered Ising Models: Comparison with Experiments", Phys. Rev. Lett. Vol.80, p.1118.
22. **Burns, G., and Bruce A. Scott, (1970)**,"Raman Spectra of Polycrystalline Solids; Application to the PbTi1-xZrxO3 System", Phys. Rev. Lett. Vol.25, p.1191.
23. **Keer, H. V., Principles of Solid State Physics**, **(1993)**, Wiley Eastern, New York.
24. **Lines, M. E., (1977),**"Microscopic model for a ferroelectric glass", Phys. Rev. B, Vol. 15, p. 388

25. **Haertling, G. H., (1999)**, "Ferroelectric ceramics: history and technology. J. Am. Ceram.Soc. Vol.82, pp.797-818.
26. **Przeslawski,J., Iglesias, T., Gonzalo,J.A., (1995),** Solid State Commun. Vol.96, p.195.
27. **Sun, X., Wang, M., Pan, Q. W., Shi, W., and Fang, C. S., (1999)**, "Study on the Growth and Properties of Guanidine Doped Triglycine Sulfate Crystal", Crystal Research and Technology, Vol.34, pp.1251-1254.

CHAPTER 2

REVIEW OF LITERATURE

2.1 Literature Survey

Inspite of the promising features of TGS crystal, such as room temperature detector operation and without any external bias, it has major disadvantage that it depolarizes by thermal, mechanical and electric means. The depolarization negatively influences the pyroelectric figure of merit [1]. In order to overcome this difficulty, several studies attempted with different dopant to achieve effective internal bias and desired ferroelectric properties of TGS crystals. Investigation on the doping of TGS crystals by amino acid [2-5] reveal that this drawback may overcome. Many researchers have investigated the properties of pure TGS single crystals and influence of amino acids, simple organic and inorganic compounds, metallic impurities, etc., on the physical and other properties of TGS single crystals [6].

Alanine dopant molecule is similar to the glycine molecule, except the CH_3 asymmetric group. Doped TGS crystals show a modified habitues versus the pure ones, mirror external shapes of L-alanine versus D-alanine doped crystals [7-8] suggest an equivalent substitution of the glycine G1 molecule in the crystal lattice [9], however, the hysteresis loops and some other characteristic data of TGS crystals, doped with racemic mixture (L+D- alanine) [10], suggest a non-equivalent substitution. L-alanine molecule substituted for glycine1 in the crystal lattice cannot be inverted upon switching because of its chiral structure. Thus L-alanine doped TGS crystal causes an internal bias field Eb and results in a macroscopic irreversible polarization in one predetermined sense of the ferroelectric b-axis [11].

The effect of amino acids doping in TGS has then studied extensively [12]. In case of lysine doped TGS dielectric permittivity and spontaneous polarization decrease with improved pyroelectric properties. In addition lysine doped TGS crystals possess higher mechanical hardness when compared to pure TGS [13]. It has also reported that L-threonine, DL-threonine, and L-methioine doped TGS results decrease of dielectric constant when compared to pure TGS. The L-threonine doped TGS has the maximum pyroelectric coefficient and hence material is suitable for detector applications [14]. Raghavan et al [15] found that the presence of optically active dopants of leucine and isoleucine increases the coercive field and decreases the spontaneous depolarization of TGS crystals, will be useful

for pyroelectric applications. Jayalakshmi and Kumar [16] have recently observed an increase of coercive field and spontaneous polarization for L-tryptophan added TGS when compared to that for pure TGS crystal. Meera et al [17] observed an increase of coercive field for L-cystine added TGS crystal. L-asparagine addition [18] increases whereas L-tyrosine addition [19] decreases the microhardness of TGS single crystal.

The study of the temperature dependence of the absorption edge of a certain substance provides a deep understanding of the interaction processes between the optical excitation (ie, electronic excitations) and the phonon spectra. In particular the measurements of the absorption edge of ferroelectrics in the vicinity of the phase transition temperature gives an opportunity to obtain information on the character of the phase transition and the nature of the chemical bonds between lattice units [20]. The admixture (addition) of transition metal ions essentially modifies the physical properties of TGS, causing bands in the ultraviolet spectral range. These bands make these crystals a candidate for short wavelength holographic recording.

E1-Fadl [21] has carried out optical absorption measurements near the absorption edge in the energy range 3 to 5.5 eV on pure TGS and TGS crystals doped with Cu2+, Mn2+ or Ni2+ in the temperature range 290 to 360°K. Temperature dependence of the band gap Eg (T) reveals an anomaly at the phase transition temperature for both pure and doped TGS crystals. The indirect allowed transition is the most probable type of transition near the fundamental edge of pure TGS and TGS crystals doped with divalent ions, and the phonon energy associated with the allowed indirect transition changes from one dopant to another. Doping of TGS crystals with small concentration of divalent ions considerably affects the measured optical parameters. The effect however, varies from one dopant to another according to their physicochemical activity. I.V. Vavresyuk et al [22] have studied changes in properties of TGS doped with metal ions.

Mihaylova and Byrne [23] have studied TGS crystals doped with Nd by Raman spectroscopy. Doping of TGS with Nd does not cause a change in the crystal structure and the symmetries of groups in the unit cell remain unaffected. A new mode at 1535cm-1 appeared for all crystals doped with Nd, which indicates that Nd is co-ordinated with the glycine molecule. Doping with Nd affects significantly the C-CO bending mode at 584 cm-1, The O-C-O bending mode at 665 cm-1, the SO4 2-mode at 1086 cm-1 and the CH2 wagging and twisting mode at 1310 cm-1. The Raman bands at 1374 and 1413 cm-1 indicate the

presence of a zwitterion, which supports Hoshino's theory for spontaneous polarization reversal in TGS.

CO2+ doped TGS crystals studied by Prokopova et al [24] have been shown to possess a very good structural quality with stabilized domain structure at room temperature. The results obtained by Novotny et al [25] on the preparation of TGS single crystals doped by palladium (especially on the growth of non-polar (001) pyramid) could be important for the growth of high-volume crystals for application purposes. Novotny et al [26] have reported the procedure of single crystal growth of full faceted TGS and deuterated TGS (DTGS) with varying content of Pt (II) and Pt (IV) ions and with L-alanine impurities in the growth solution. They measured in great detail the main physical properties of prepared LATGS / Pt (IV) and LADTGS / Pt (II) singles crystals such as spontaneous polarization PS, values of coercive fields EC, Internal electric field Eb, dielectric permittivity εr and dielectric losses tan δ. Their results suggest that the prepared modified TGS single crystals are suitable material for preparation of high sensitivity broad area infrared detectors.

Muralidharan et al [27] have reported the rare earth ions dopants La, Ce and Nd on the growth aspects and ferroelectric properties of TGS single crystals. The dopants significantly modify the morphology of the crystals. Dielectric measurement revealed that the dielectric constant of Ce doped TGS increases rapidly at the transition temperature. Well – structured rectangular hysteresis loop have been observed for all the doped crystals. Lenticular ferroelectric domain patterns were observed on the (010) plane of the grown crystals. La doped TGS crystals possess a high Tc and coercive field values. Among the three dopants, Nd doped TGS possesses low dielectric constant and high pyroelectric coefficient suggesting that this can be a potential material for infrared detectors. Sun et al [28] have grown guanidine doped TGS crystal and found that this crystal has better pyroelectric properties than those of pure TGS crystal.

Chang et al [29] have reported the growth and properties of TGS crystals doped with urea. It was found that the normalized growth yield and pyroelectric and dielectric constants could be increased significantly by urea addition. TGS crystals doped with 5 and 10 wt% urea exhibited upto five times higher material figures of merit for infrared pyroelectric detectors compared with undoped TGS crystals. The Vicker's hardness of doped crystals increased with urea content to about three times the undoped value in the (010) direction at 10% urea. No significant increase in the hardness was found, however, in the (001) direction.

Based on Devonshire [30] thermodynamic theory the relationship $\lambda/X = Ps/C$ can be obtained and can be regarded as a method to increase the pyroelectric material figure of merit of ferroelectric crystals. Shi et al [31] have grown modified TGS crystals doped with urea or co-doped with urea and other dopants and investigated the pyroelectric properties. The pyroelectric figures of merit $M(\lambda/\varepsilon r)$ of the doped TGS crystals are obviously higher than those of pure TGS.

Meera et al [32] have grown and characterized thiourea doped TGS crystals. Dielectric studies show a shift in the curie temperature because of doping pyroelectric coefficient was found to be increased due to thiourea addition on TGS. Very recently, Krishna kumar et al [33] have grown thiourea doped TGS single crystals and subjected them to X-Ray diffraction, FTIR and Raman spectroscopic and optical absorption measurements. The powder technique of Kurtz and Perry confirmed the non-linear optical (NLO) property of the grown crystals. The shift and the appearance of additional wave number in the IR and Raman spectra of doped crystal establish the co-ordination of thiourea with TGS in the lattice. The results of the response of the mechanical behaviour of thiourea doped TGS crystal will have significant effect on machining the crystal for device purpose. From the results of optical transmission it was found that the doped crystal exhibit excellent transmission in entire UV-Visible range studied than undoped crystal. This property enables the material for thefabrication of IR detectors and in some optoelectronics device technology. Also sufficient shift in the lower cut off wavelength towards UV region in doped crystal makes this material to find application in generation of UV light. Higher second harmonic generation (SHG) efficiencies were observed for pure (52.5 mV) and thiourea doped (60.2 mV) TGS crystals when compared to that for potassium dihydrogen orthophosphate, KDP (15 mV).

Many metallic dopants modified the properties to some extent, but in general they have been found ineffective for achieving the desired changes in the properties [34]. Metallic ions like Fe^{3+} and Cr^{3+} ions changed the crystal growth characteristics, but decreased the pyroelectric coefficient and spontaneous polarization [35]. Li^{+} and Mn^{2+} modified the growth habit and produced a high pyroelectric coefficient, but the high dielectric constant value did not affect the pyroelectric material figure of merit $(P/\varepsilon r)$, where P = pyroelectric coefficient, εr = dielectric constant [36]. Ni^{2+} ions at a concentration level of 10% by weight in the solution increased the pyroelectric figure of merit but did not enhance the crystal

growth rate , whereas Mg2+ and Cu2+ modified the growth habit but marginally increased the pyroelectric material figure of merit .

Phosphoric acid (H3PO4) as a dopant has been found to yield crystals with a large 'ac' plane area useful for IR detector applications [37]. Even at a very low concentration level of H3PO4, a significant improvement in the pyroelectric coefficient, lowering of the dielectric permittivity at transition temperature (Tc) and increase in the coercive field of the TGS crystal have been reported [38]. The replacement of sulphur by phosphorous in the lattice introduces asymmetry in the P-E hysteresis loop [39]. It has also been found that the concentration of H3PO4 is critical for achieving the desired material properties for commercial IR detector applications [40].

Very recently, Balu et al [41] have grown ammonium dihydrogen orthophosphate (ADP) doped TGS single crystals and characterized. X-Ray analysis showed a slight variation in the lattice parameters for doped crystals. The optical transmission spectra indicated a wide optical transparency in the entire visible and near IR region. Dielectric measurements revealed a shift of curie point to lower temperature with increase in dopant concentration. Microhardness studies have shown that the hardness decrease with increase in ADP concentration. Nakatani [42] has studied temperature independent internal bias field in L-α-alanine doped TGS crystal. Serna et al [43] has studied the positron life time spectra of pure and L-alanine doped TGS.

Arunmozhi et al [44] have studied the effect, of anti- ferroelectric ADP with TGS crystals. They shown that inhomogeneous incorporation of dopants gives rise to a distribution in coercive fields in the different growth sectors. The incorporated dopant hinders polarization switching, which results in the increase in coercive field. N.Theresita Shanthi et al [45] have grown sodium bromide doped TGS single crystal from aqueous solution. They shown that the dopant addition increases the hardness number for low concentration and decreases the hardness when the concentration is high, they also show that there is no change in the curie point temperature due to dopant addition. Copper sulphate doped TGS crystal were grown by K.Balasubramanian and P.Selvarajan [46]. They observed that the dielectric parameters increased when the TGS crystal are doped with copper sulphate. They also noticed that there was an increase of microhardness number when TGS crystal was doped with copper sulphate. Farhana Khanum and Jiban Podder [47] have studied the effect of nickel sulphate doped TGS crystals. They found that the lattice parameters are slightly distorted due to the incorporation of nickel ion into the lattice size of the TGS crystal,

M.Costache et al [48] have grown alanine doped TGS crystal in the pyroelectric phase. They found that remarkable asymmetry of measure pyroelectric coefficient of d and L-alanine doped TGS crystal. Suggest a non-equivalent substitution of glycine in host lattice. Farhana Khanum and Jiban Podder [49] have doped potassium bromide with TGS and they shown that the doped crystal have wide optical transparency in the entire visible region. K.Balasubramanian et al [50] have grown TGS crystal in CdS nano particle dispersed water by solution method and studied the effect of Cd2+ ions. Alexandru and Ann NY [51] has studied the effect of D-alanine in TGS crystal in the dielectric parameters. They found that the relaxation time is not a real constant on such large time interval. In a semi long scale, permittivity shows three stages, probably related to several mechanism of relaxation. A.J.Jeya Prakash Manoharan et al [52], have studied the effect of amino acid in TGS crystal. They found that the D.C conductivity increases with temperature as well as dopant concentration.

Farhana Khanum and Jiban Podder [53] have studied that effect of LiSO4 on TGS crystal. They found that the D.C conductivity increases with temperature as well as dopant concentration and also shown that the curie point temperature remain same for pure and doped crystal. But the dielectric constant and loss factor increases with doped concentration grown by n bromo succinide added TGS crystal were grown by Rai and his co workers [54]. They found that, the dielectric constant of NBSTGS crystal decrease with the increase in NBS concentration and considerable shift in the phase transition temperature (Tc) towards the higher temperature.

2.2. Present work

Today, crystals are the pillars of the modern technology, without crystals there would no electronic industry, no photonic industry, no fiber optics communication, very little modern optical equipment. Pure as well as mixed and doped crystals are grown in every day in large quantities due to the increased need of crystals in solid state devices TGS is the order – disorder type ferroelectric crystal. Since the discovery of its ferroelectric nature in 1956 by Mathias, TGS is one of the best studied ferroelectric materials TGS exhibits good pyroelectric properties and finds wide application as pyroelectric detectors. It shows second – order phase transition at curie point temperature (Tc = 49°C) [55].

In the present study, TGS was synthesized from glycine and sulphuric acid, pure, Potassium dihydrogen orthophosphate (KDP) and Ammonium dihydrogen orthophosphate (ADP) mixed single crystals of TGS were grown by slow evaporation technique. Totally,

seven crystals (1 pure TGS, 3 TGS mixed KDP , and 3 TGS mixed ADP) were grown in identical condition. The concentration of KDP in the TGS mixed KDP crystal and TGS mixed ADP were determined from EDAX spectrum taken. Powder X-Ray diffraction data were collected for the seven samples and they were indexed using the standard methods, particle size were also determined. Optical measurements like UV – Visible and FTIR studies have been carried out for all the seven grown crystals. The results obtained and detailed report of present research work are provided in this report which is organized as follows. The topic of research is introduced in the first chapter. The detail explanation of the synthesis of sample TGS crystal, TGS-KDP and TGS-ADP mixed crystals chemical characterization along with the results and discussions are discussed in chapter three and four. Summary, conclusion and future scope are given in chapter five. References are provided in each chapter .

2.3 REFERENCES

1. N.Nakatani,Jpn.J.Appl.Phys. **(1991),** 30, 1024
2. S.Aravazhi, R.Jayavel, C.Subramanian, Ferroelectrics **(1997),** 200, 279
3. G.Su, Y.He, H.Yao, Z.Shi, Q.Eu, J.Cryst, Growth, **(2000),** 209, 220
4. K.Biedrzycki, Solid State Commun. **(2001),** 118, 141
5. Ravi G.,Arunmozhi. G.,Aravazhi .S., Anbukumar.S., Ramasamy.P, Proc. 4th Int. Conf. on Prop & Appl.of dielectric materials, Brisbane, Australia, **(1994),** P.247, 249
6. K.Meera, R.Muralidharan, P.Santhana Raghavan, R.Gopalakrishnan and P.Ramasamy, J.Cryst. Growth **(2001),** 226, 303
7. B.Brezina and M.Havrankova, Cryst.Res.Technol. **(1985),** 20, 787
8. B.Brezina and M.Havrankova, Cryst. Res. Technol. **(1995),** 20, 781
9. E.T. Keve, K.L.Bye, P.W.Whipps and A.D.Annis, Ferroelectrics **(1971),** 3, 39
10. H.V.Alexandru and C.A. Berbecaru, Ferroelectrics, **(1997),** 202, 173
11. Z.Zikmund and J.Fousek,Phys.Stat.Sol.(a) **(1989)** 112, 625
12. S.Aravazhi, R.Jayavel, C.Subramanian, Ferroelectrics **(1997),** 200, 279
13. K.Meera, R.Muralidharan, A.K.Tripathi, R. Dhanasekaran and P.Ramasamy, J.Cryst. Growth, **(2004),** 260, 414
14. K. Meera, R. Muralidharan, A.K.Tripathi and P.Ramasamy, J.Cryst. Growth **(2004),** 263, 524.
15. C.M.Raghavan, R.Sankar, R.Mohan Kumar and R.Jayavel, Mater. Res. Bull. **(2008),** 43, 305
16. D.Jayalakshmi and J.Kumar, J.Cryst. Growth, **(2008),** 310, 1497

17. K.Meera, R.Muralidharan, P.Santhana Raghavan, R.Gopalakrishnan and P.Ramasamy, J.Cryst. Growth **(2001),** 226, 303.

18. S.Kalainathan, M.Beatrice Margaret and T.Irusan, Cryst.Eng **(2002),** 5, 71

19. K.Meera, S.Aravazhi, P.Shanthana Ragavan and P.Ramasamy, J.Cryst. Growth, **(2000),** 211, 220

20. P.Pacesova, B.Brezina and L.Jastrabik, Phys.Stat.Sol.(b) **(1983),** 116, 645

21. A.A. El-Fadl, J.Phys. Chem.Solids **(1999),** 60, 1881

22. Vavresyuk.I.V, Milovidova.S.D, Evseev.I.I, Crystallography Reports, **(1996),** 41, 540-1

23. E.M.Mihaylova and H.J. Byrne, J.Phys. Chem. Solids **(2000),** 61, 1919

24. L.Prokopova, J.Novotny, Z.Micka and V.Malina, Cryst. Res. Technol. **(2001),** 36, 1189

25. J.Novotny, L.Prokopova and Z.Micka, J.Cryst. Growth **(2001),** 226, 333

26. J. Novotny, B.Brezina and J.Zelinka, Cryst.Res. Technol. **(2004),** 39, 1089

27. R.Muralidharan, R. Mohankumar, R.Dhanasekaran, A.K.Tripathi, R.Jayavel and P. Ramasamy, Mater. Lett **(2003),** 57, 3291.

28. X.Sun, M. Wang, Q.W.Pan, W.Shi and C.S.Fang, Cryst. Res. Technol **(1999),** 34, 1251

29. J.Chang, A.K. Batra and R.B.Lal, J.Cryst. Growth **(1996),** 158, 284

30. A.E. Devonshire, Adv.Phys. **(1954),** 3, 85

31. W.Shi, M.Wang, X.Sun, Q.T. Gu, H.S.Zhuo and C.S. Frang, Prog. Cryst.Growth & Charact. Mater **(2000),** 40, 293

32. K.Meera, R.Muralidharan, A.K.Tripathi, R. Dhanasekaran and P.Ramasamy, J.Cryst. Growth, **(2004),** 260, 414

33. V.Krishnakumar, S.Sivakumar, R.Nagalakshmi, S.Bhuvaneswari and M.Rajabhoopathi, Spectrochimica Acta A (in press), **(2009)**

34. M.A.Gaffar, A.A.El-Fadl Indian J.Pure & Appl.Phys **(1988),** 26, 28

35. M.A.Gaffar, A.Abu El-Fadl and S.A.Mansour, J.Phys. D:Appl.Phys **(1989),** 22, 327

36. A.S.Bhalla, C.S. Fang, L.E.Cross and Y.Xi, Ferroelectrics **(1984)** 54, 151

37. A.Saxena, V.Gupta and K.Sreenivas, Mater. Sci. Eng. **(2001),** B79, 91

38. Y.Kim and G.Park, Ferroelectrics **(1993),** 146, 99

39. N.Nakatani and M.Yoshio, Jpn.J.Appl.Phys, **(1996)** 35, 5752

40. C.S.Fang, Y.X-i, A.S. Bhalla and L.E. Cross, Ferroelectrics, **(1983),** 51, 9

41. T.Balu, T.R.Rajasekaran and P.Murugakoothan, Curr.Appl.Phy.(in press) **(2009)**

42. Nakatani. N., Jup.J. Appl.Phys., **(1990),** 29, 2038-40

43. Serna.J., Ferroelectries, **(1992),** 129, 157-63

44. G.Arunmozhi, S.Lanceros-Mendez, E.de matos Gomes, Materials letters **(2002),** 54, 329-336

45. N.Theresita Shanthi, P.Selvarajan and C.K.Mahadevan, Indian Journal of Science and Technology **(2009),** 2, 3

46. K.Balasubramanian, P.Selvarajan, Recent Research in science and Technology **(2010),** 2, 3

47. Farhanakhanum, Jiban Podder; Journal of crystallization process and Technology **(2011),** 1, 49-54

48. M. Costache, I.Matei, L.Pintilie, H.V.Alexandru, C.Berbecaru, Journal of Optoelectronics and Advanced Materials **(2001),** 3, 75-81

49. Farhanakhanum, Jiban Podder; Journal of crystallization process and Technology **(2011),** 1, 26-31

50. K.Balasubramanian, P.Selvarajan, and E.Kumar, Indian Journal of Science and Technology **(2010),** 3, 1

51. Alexandru. H.V, Ann NY, Acad Sci **(2009),** 387-96

52. A.J.Jeyaprakash Manoharan, N.Josephjohn, V.Revathi, K.V.Rajendran and P.M.Andavan, Indian Journal of Technology, **(2011),** 4, 6

53. Farhana Khanum and Jiban Podder, Hindawi Publishing Corporation, International Journal of Optics, **(2012),** 2012

54. Rai Chitharanjan, Byrappa.K, Dharmaprakash.S.M, Physica B; Physics of condensed Matter **(2011)** 408, 3308-3312

55. Ravi G.,Arunmozhi. G.,Aravazhi .S., Anbukumar.S., Ramasamy.P, Proc. 4th Int. Conf. on Prop & Appl.of dielectric materials, Brisbane, Australia, **(1994),** P.247, 249.

CHAPTER 3

Growth and Characterization of Triglycine Sulphate (TGS) Crystal mixed with Potassium dihydrogen Orthophosphate (KDP)

3.1 Introduction

Triglycine sulphate (TGS) is a ferroelectric crystal. The ferroelectric crystals find important applications in optoelectronics, photonics and used in the fabrication of high sensitivity infrared detectors at room temperature. TGS was synthesized by taking the AR grade Glycine (CH_2NH_2COOH) and concentrated sulphuric acid (H_2SO_4) in the molar ratio 3:1 respectively. The synthesized pure TGS is mixed with Potassium dihydrogen Orthophosphate (KDP) in the molar ratio (9:1), (8:2) and (7:3) and the crystals were grown from aqueous solution by slow evaporation method at room temperature. The chemical composition of the grown crystals is confirmed by Energy Dispersive X-ray Analysis (EDAX). The solubility of grown crystals is determined using water as a solvent. The solubility curve shows that the TGS mixed with KDP has higher solubility than the pure TGS. The grown crystals were crushed to a uniform fine powder and subjected to XRD analysis. Appearance of sharp peaks confirms the good crystalline nature. Using Debye-Scherer's equation (D-S) particle size has been calculated. The Second harmonic generation efficiency is determined by Kurtz powder technique. The KDP crystal is used as a reference material, it is found that the relative SHG conversion efficiency of the grown crystals is greater than KDP sample which indicates the suitability of crystals for various applications. Optical transmission spectra are recorded for the crystals in the wavelength region 200 to 1100 nm using Perkin-Elmer Lambda 35 UV-Vis spectrophotometer. The electronic band transitions is studied from the plot of $(\alpha h\nu)^2$ versus photon energy (hv) and the band gap energy has been calculated. The functional groups have been identified by Fourier Transform Infrared spectroscopy (FTIR). The experimental results evidence the suitability of the grown crystals for optoelectronic applications.

Triglycine Sulphate crystals have technological importance for room-temperature infrared detectors, earth exploration, radiation monitoring and astronomical telescopes. TGS undergoes a second-order ferroelectric phase transition at Curie temperature $T_C = 49^0C$, ferroelectric and pyroelectric materials are polar and possess a spontaneous Polarization. However, this polarity can be reversed through the application of an electric field with

ferroelectric materials [1-4]. They are similar to ferromagnetic materials in that they exhibit hysteresis loops. This material has found application in the fabrication and development of infrared detectors due to its high pyroelectric coefficient (p), reasonably low dielectric constant and best figure-of-merit. TGS crystals have been focused in various aspects such as growth rate, structural modification, pyroelectric, mechanical, optical and ferroelectric properties. Also the crystals are of particular interest for the photo induced nonlinear optical effects. TGS has a tendency to depole, which can be prevented by suitably mixing optically active molecules in the glycine site of TGS.

This chapter describes the Solubility, crystal growth, structural, Optical, and SHG efficiency of Triglycine sulphate (TGS) mixed with Potassium dihydrogen Orthophosphate (KDP) in the molar ratio 9:1, 8:2 and 7:3 grown by slow evaporation method. The effects of mixing KDP crystals on the quality and performance of the crystals are analyzed. The results of the TGS mixed with KDP crystals are compared with the pure TGS crystals.

3.2 Significance of the study

TGS is important for understanding the physics of the ferroelectric phenomenon as well as for its applications. Despite its complicated chemical and crystallographic form, it is being studied for several years mainly for two reasons: Firstly, its excellent pyroelectric properties and high figures of merits make it suitable for use in the low-power detector applications where high detectivities are required, e.g. in the set up of spectrometers.

Secondly, it is one of the very few ferroelectrics known to exhibit a typical second-order order-disorder type of phase transition, offering a spectrum of possibilities for understanding the basic mechanism of group-subgroup type of phase transitions in crystalline solids.

3.3 Methodology

3.3.1 SYNTHESIS

Triglycine sulfate (TGS) was synthesized by taking glycine and sulfuric acid in the molar ratio 3:1. $3(NH_2CH_2COOH) + H_2SO_4 \rightarrow (NH_2CH_2COOH)_3.H_2SO_4$.

The required amount of sulfuric acid was diluted with triple distilled water. Then the calculated amount of glycine was added and dissolved in dilute H_2SO_4. The solution was heated until the salt crystallized. Extreme care was taken during crystallization to avoid the oxidation of glycine.

3.3.2 CRYSTAL GROWTH

Analytical reagent grade (AR) samples of potassium dihydrogen orthophosphate ($KH_2PO_{4)}$ was mixed with TGS in the molar ratio (9:1), (8:2) and (7:3) separately and dissolved in a triple distilled water. The solution was stirred well for six hours constantly using magnetic stirrer, then solution was filtered using Whatmann paper as shown in Figure 1.

Figure 1. Solution stirred using Magnetic Stirrer and Filtering action

The resulting solution is kept in a Petri dish and covered for crystallization at room temperature by slow evaporation method. The spontaneous nucleation took place in two days and crystals of size 2mm x 2mm were grown within two weeks as shown in Figure 2. To get the good transparent crystals, the crystals were crushed and kept for recrystallization, So that its transparency and shape was improved.

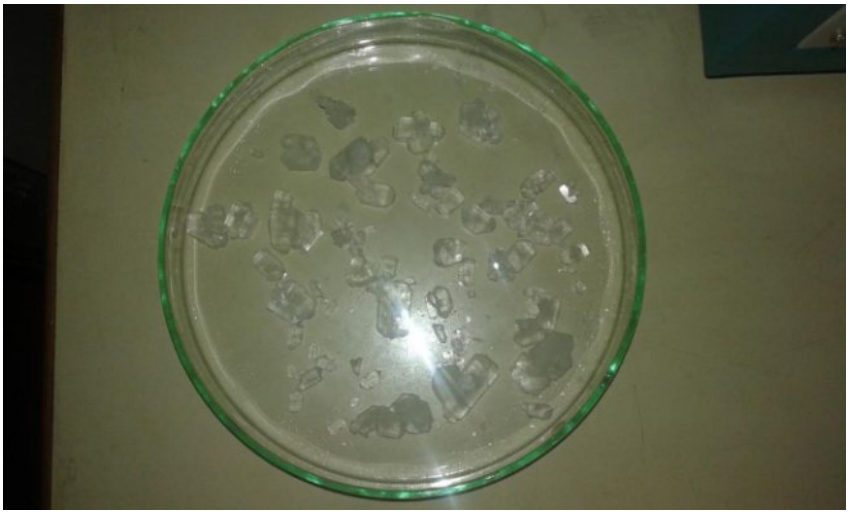

Figure 2. Shows the Crystals grown by Slow Evaporation method.

Pure TGS, TGS-KDP mixed crystals are also grown using Constant temperature bath as shown in Figure 3. In this method the temperature is fixed constant at 35^0C and provision is made for evaporation of solvent. Typical growth conditions involve temperature stabilisation to about +/- 0.005^0C. This evaporation technique of crystal growth has the advantage that the crystals grow at a fixed temperature.

Figure 3. Crystals grown at constant Temperature using Constant temperature bath.

Optically good quality large-size single crystals were obtained in a period of 30 days. All the grown crystals were found to be very stable and transparent. The grown crystals are shown in the figure 4-7.

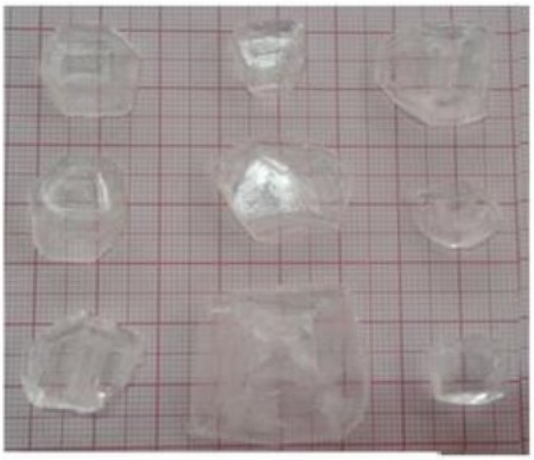

FIGURE 4. Photograph of as grown Pure TGS Single crystals

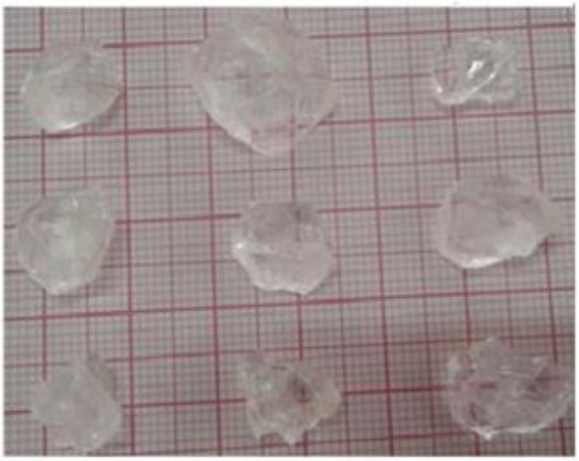

FIGURE 5. Photograph of as grown TGS mixed KDP (9:1) Single crystals

FIGURE 6. Photograph of as grown TGS mixed KDP (8:2) Single crystals

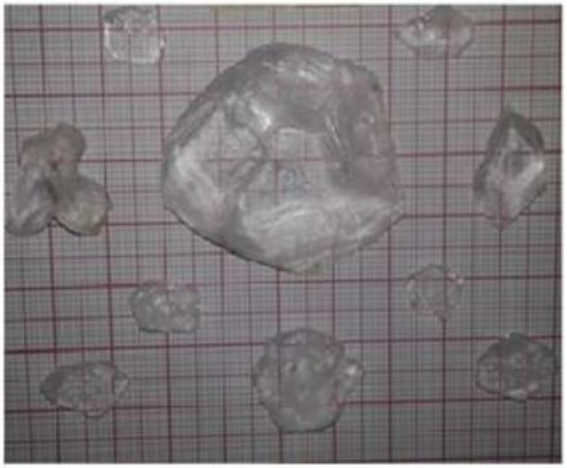

FIGURE 7. Photograph of as grown TGS mixed KDP (7:3) Single crystals

3.4 RESULTS AND DISCUSSION

3.4.1 Energy Dispersive X-ray Analysis (EDAX)

In order to confirm the presence of KDP in pure TGS crystals, the sample of grown crystals were subjected to Energy Dispersive X-ray Analysis. Figures 8a-8c shows the EDAX data of TGS:KDP mixed crystals. From the EDAX and XRAD data, it is confirmed that the KDP has gone into the lattice of the TGS crystals.

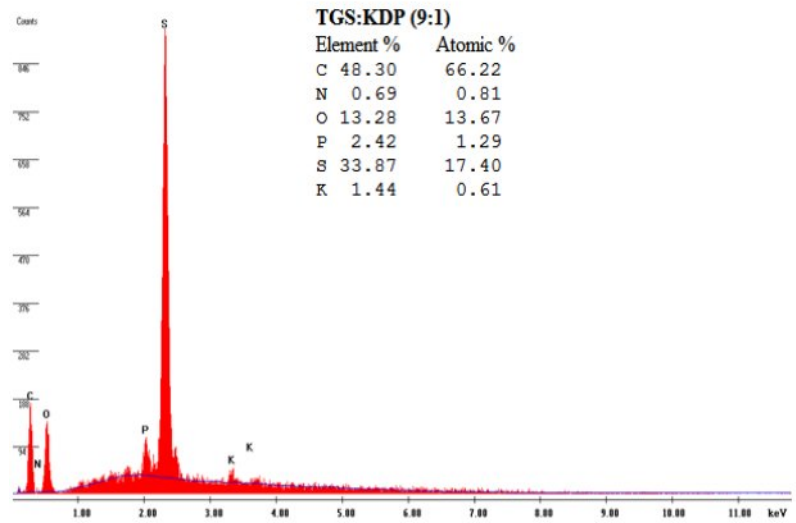

FIGURE 8a. EDAX Spectra of TGS:KDP (9:1) grown crystal

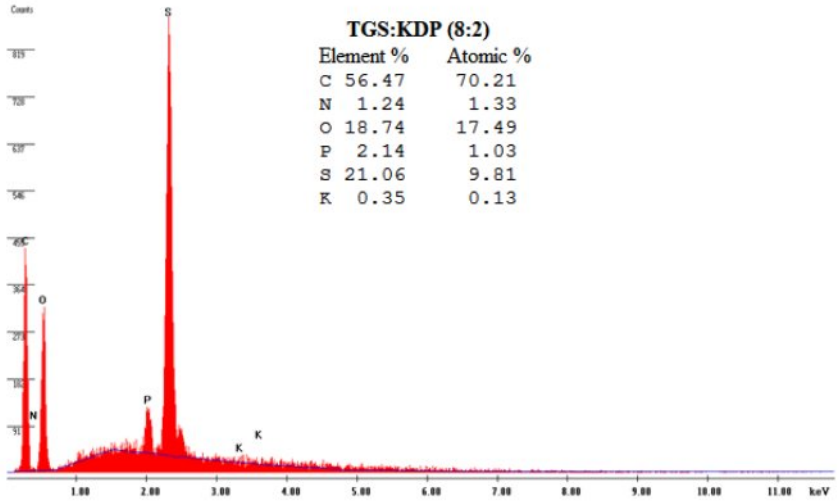

FIGURE 8b. EDAX Spectra of TGS:KDP (8:2) grown crystal

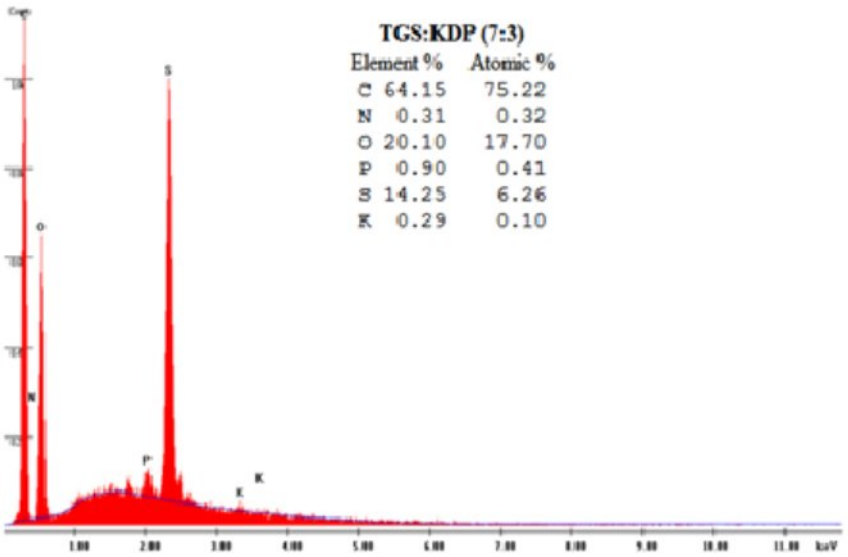

FIGURE 8c. EDAX Spectra of TGS:KDP (7:3) grown crystal

3.4.2 Determination of Solubility

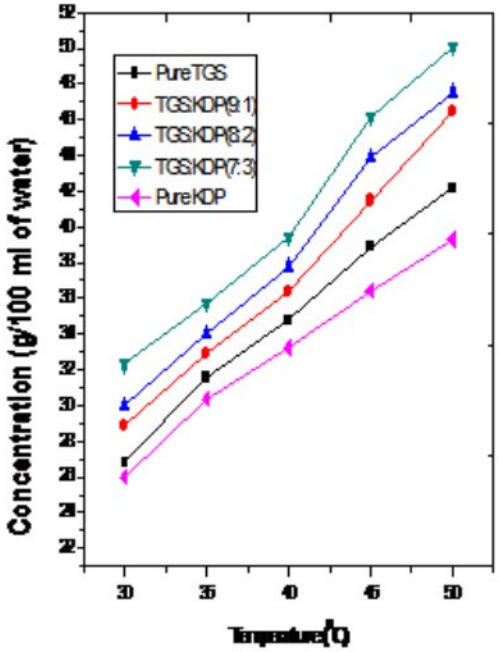

FIGURE 9. Solubility Curve of the grown crystals

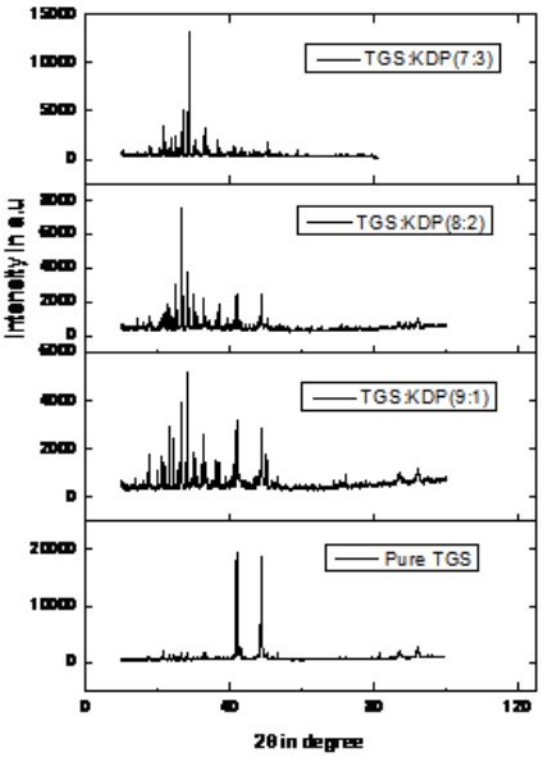

FIGURE 10 Powder X-ray diffraction patterns of grown crystals

The Solubility studies were carried out in a constant temperature water bath (CTB). The solution was stirred continuously for 6 hours to achieve stabilization using an immersible

magnetic stirrer. Solubility was determined by gravimetric analysis for different temperatures (30–50^0 C). The solubility curve of pure TGS, pure KDP, TGS mixed with KDP is shown in Figure.9. It is observed from the solubility curve that the solubility of TGS mixed with KDP increases with increase in the molar wt of KDP and with respect to pure TGS and pure KDP and has positive temperature co-efficient.

3.4.3 XRD Analysis

Good quality grown crystals were crushed to a uniform fine powder and subjected to XRD analysis using XrdwinPD 4-dectris computer based diffractometer with a characteristic Cu Kα (1.540598) radiations from 10^0 to 100^0 at a scan rate of 10^0/min. Appearance of sharp peaks confirms the good crystallinity of the grown samples. The observed values are in good agreement with the reported values [5-6]. The XRD spectra of pure TGS and KDP mixed TGS crystals are shown in Figure 10. Using Debye - Scherer's equation (D-S) particle size has been calculated and is given in the Table 1.

TABLE 1. Particle Size Calculated by Debye-Scherer's (D-S) equation.

Sample (Crystals)	Average Particle Size (nm)
Pure TGS	26.784
TGS:KDP (9:1)	37.97618
TGS:KDP (8:2)	44.5836
TGS:KDP (7:3)	52.3744

Table 2. SHG Signal and SHG efficiency of grown crystals

Details of the sample	SHG Signal	SHG Efficiency w.r.t KDP	SHG Efficiency w.r.t TGS
Pure TGS	98mV	1.225	1
TGS:KDP (9:1)	81mV	1.0125	0.826
TGS:KDP (8:2)	78mV	0.975	0.795
TGS:KDP (7:3)	89mV	1.112	0.908

3.4.4 Optical transmission studies

Crystal plates of pure TGS and KDP mixed TGS crystals were cut and polished without any coating for optical measurements. The dimensions of the crystals were 10x10x5mm^3. Optical transmission spectra were recorded for the crystals in the wavelength region 200 - 1100 nm using Perkin-Elmer Lambda 35 UV-Vis spectrometer. The recorded UV-Vis spectrum is shown in the Figure 11.

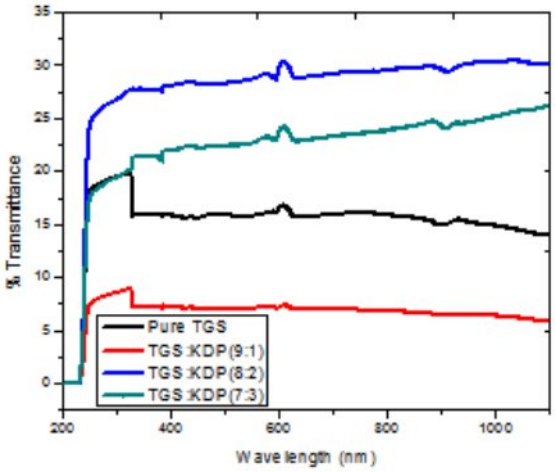

FIGURE 11 UV-Vis transmittance spectra of grown crystals

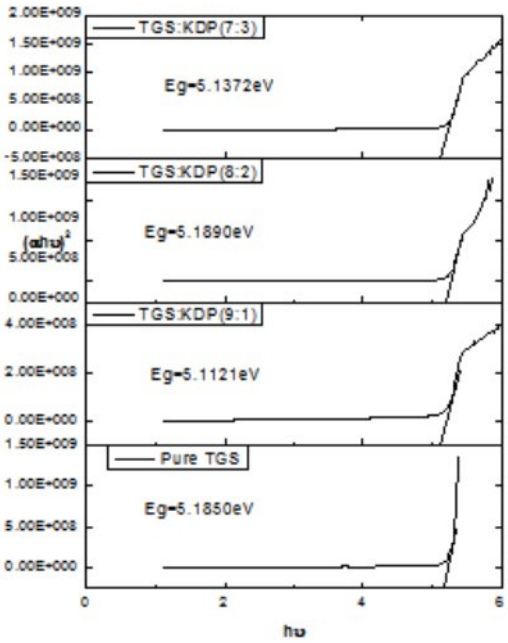

FIGURE 12 $(\alpha hv)^2$ versus photon energy hv of the grown crystals

Good optical transmittance and lower cut off wavelength are very essential properties for nonlinear optical (NLO) crystals [7]. It is observed from the figure that the Pure TGS shows 19% of transmittance, TGS mixed KDP (8:2) shows 29% and TGS mixed KDP (7:3) shows 26% of transmittance. The large transmission in the entire visible region enables it to be a good material for electro-optic and NLO applications. The above results indicate that the addition of KDP to pure TGS increased the transmittance. The plot of $(\alpha hv)^2$ versus photon energy hv as shown in Figure 12. The wide optical band gap of TGS:KDP mixed crystals is found to be 5.1121eV, 5.1890eV and 5.137eV for the molar ratio (9:1), (8:2) and (7:3) respectively suggests its suitability for optoelectronics applications.

3.4.5 FTIR Spectroscopy

The Fourier transform infrared (FTIR) spectra for the powder samples of the grown crystals was recorded in the frequency region 400 - 4000 cm^{-1} using Perkin Elmer spectrometer. The FTIR spectra of pure TGS and TGS-KDP mixed crystals are shown in Figures 13-16.

The mid IR spectrum of TGS shows a broad envelope between 1800 and 2800cm^{-1}. It includes the OH stretch of hydrogen bonded carboxyl groups, the asymmetric stretching mode of NH_3^+ at 3135.386cm^{-1} and CH_2 stretching modes just below 3000 cm^{-1}. The broadening that extends between 2800 and 2200cm^{-1} includes overlapping of bands due to the

stretching modes of hydrogen bonded NH^{3+} overtones and combination bands. The C=0 stretch of carbonyl groups display its characteristic peak at 1701.972 cm^{-1}. The CH_2 bending modes of glycine are located at 1374.381cm^{-1} and1423.164cm^{-1}. The NH_3^+ displays its characteristic bending modes at 1423.164, 1491.936 and 1529.171cm^{-1}. The intense and sharp peaks position between 900 and 1000cm^{-1} are assigned to stretching modes of carboxyl and sulphate ions. The peaks due to NH_3^+ oscillation are seen at 895.083, 862.292 and 674.687cm^{-1}. Table 3. shows the vibrational frequencies corresponding to the band assignments of pure TGS and TGS:KDP mixed crystals. The following vibrational assignments showed the hydrogen bonding extends throughout the TGS mixed KDP molecules. These hydrogen bonding results in the modification of stretching frequencies of O-H group of TGS and the carboxyl group of KDP molecules [8]. This confirms the presence of KDP in the pure TGS crystal.

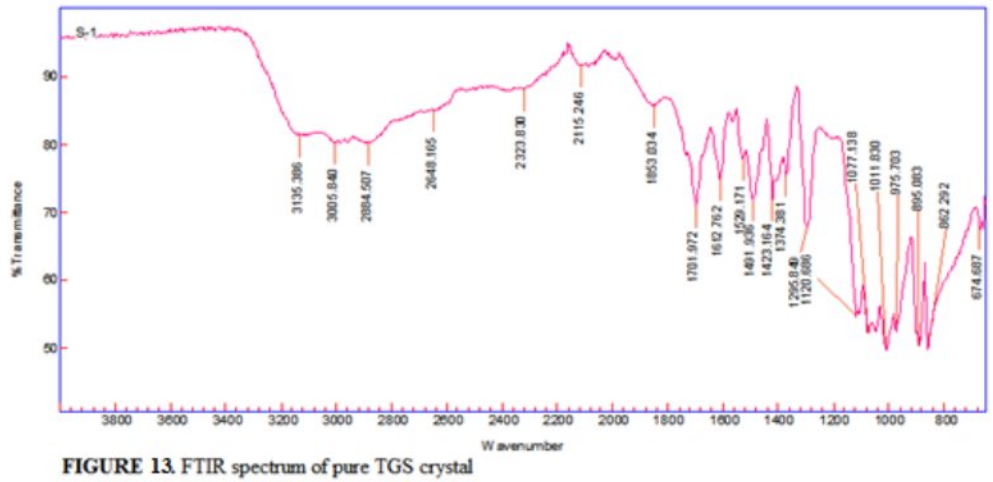

FIGURE 13. FTIR spectrum of pure TGS crystal

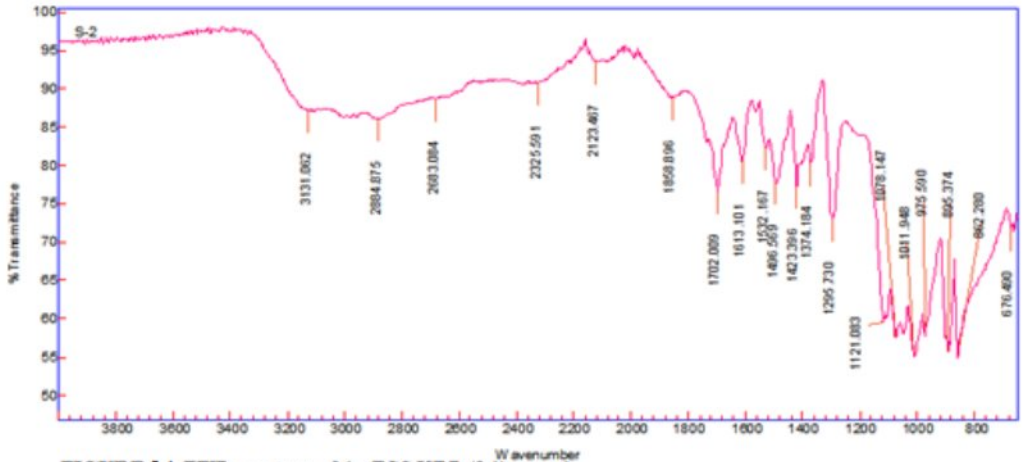

FIGURE 14. FTIR spectrum of the TGS:KDP (9:1) crystal

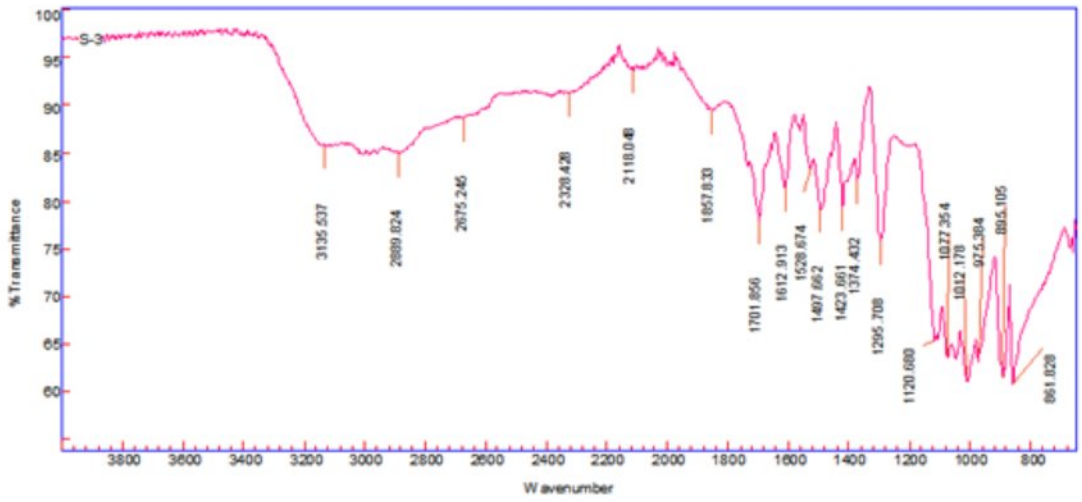

FIGURE 15 FTIR spectrum of the TGS:KDP (8:2) crystal

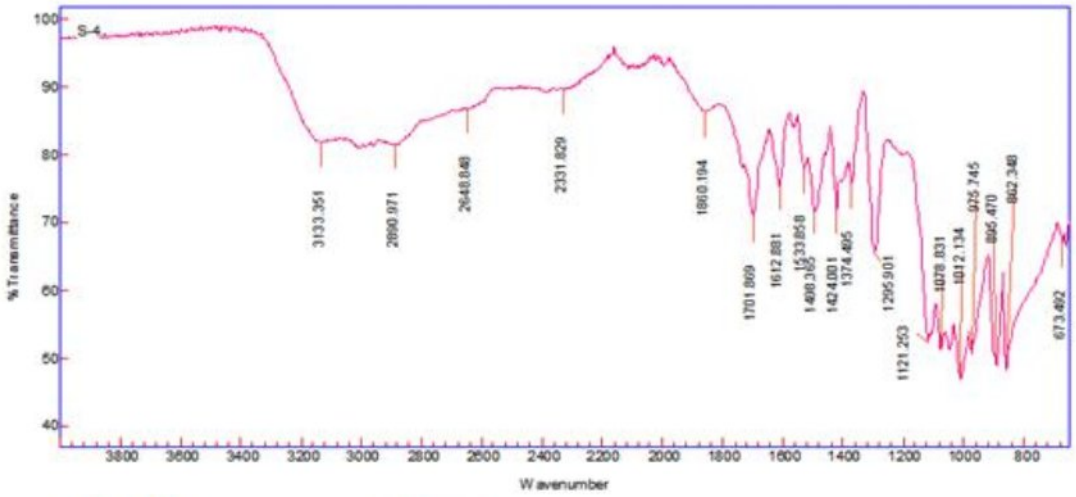

FIGURE 16 FTIR spectrum of TGS:KDP (7:3) crystal

Table 3. Vibrational frequencies for Pure TGS and TGS mixed KDP crystals

Pure TGS	**TGS:KDP (9:1)**	**TGS:KDP (8:2)**	**TGS:KDP (7:3)**	**Assignments**
3135.386	3131.602	3135.537	3133.351	O-H stretching, H-bonded
3005.840	--	--	--	O-H stretching
2884.507	2884.875	2889.824	2890.971	O-H stretching
2648.165	2683.084	2675.245	2648.848	Intermolecular H-bonded OH streching
2323.830	2325.591	2328.428	2331.829	C-H stretching
2115.246	2123.467	2118.048	--	O-H Stretching
1853.034	1858.896	1857.833	1860.194	P-O-H symmetric stretching

1701.972	1702.009	1701.856	1701.869	O-P-OH symmetric stretching
1423.164	1423.396	1423.661	1424.001	O-H stretching
1374.381	1374.184	1374.432	1374.495	CH_2 bending, P=O symmetric stretching
1011.830	1011.948	1012.178	1012.134	P-O-H symmetric stretching
975.703	975.590	975.384	975.745	O=P-OH bending
895.083	895.374	895.105	895.470	HO-P-OH bending
862.292	862.280	861.828	862.348	P-OH deformation/K-O stretching
674.687	676.490	--	673.492	PO_4 stretching

3.4.6 Second Harmonic generation Studies (SHG)

The Second harmonic generation efficiency was determined by Kurtz powder technique [9]. Laser beam coming from the source has very high energy. Its intensity is reduced by using glass plates and Neutral density (ND) filter which reduces the intensity and it allows only 1064nm wavelength to incident on the sample taken in a microcapillary tube. Output from the sample is passed through the monochromator which is intensified by photomultiplier tube and finally the signal is observed and read on the Oscilloscope. A Q-switched Nd:YAG laser beam of wavelength 1064nm and 8ns pulse width with an input rate of 10Hz was used to test the NLO property of the sample. The second harmonic signal of 532nm green light was collected by a photomultiplier tube [10]. The optical signal incident on the PMT was converted into voltage output at the cathode ray oscilloscope as shown in Figure 17.

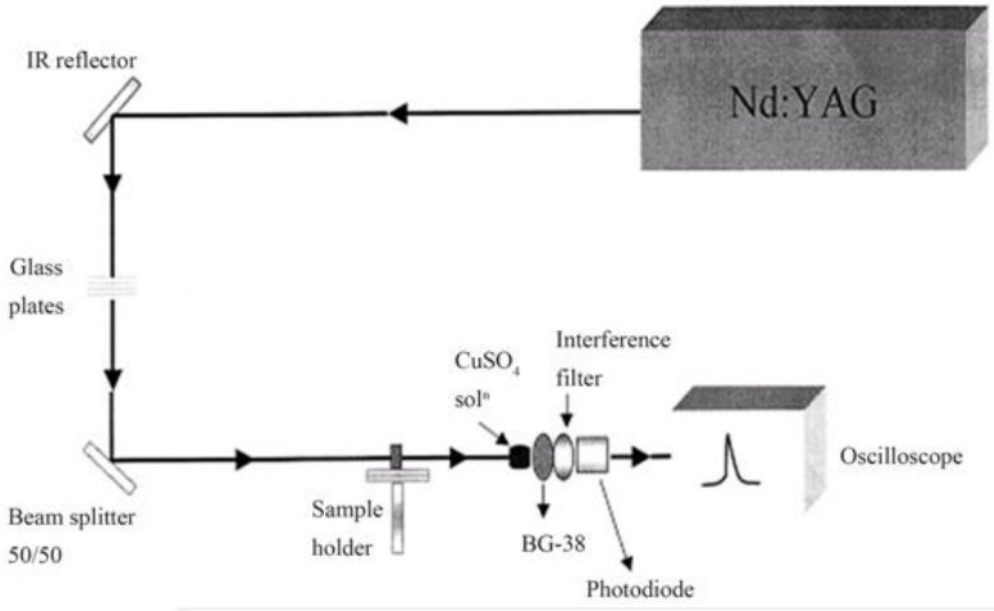

Figure 17. Schematic experimental setup for SHG efficiency measurement.

The grown crystals were crushed into fine powder and tightly packed in a microcapillary tube. It was mounted in the path of Nd-YAG laser beam of energy 5mJ/pulse. The KDP crystal was used as a reference material. The transmitted beam voltage for pure KDP was 80mV, for the pure TGS crystal 98mV, 81mV for TGS:KDP (9:1). 78mV for TGS:KDP (8:2) and 89mV for TGS:KDP (7:3) sample. It is found that the SHG efficiency of the TGS:KDP (9:1) mixed crystal is 1.0125 times greater than KDP, TGS:KDP (8:2) is 0.975 times greater than KDP and TGS:KDP (7:3) is 1.112 times greater than KDP. The measured values are given in Table 2. The relative SHG efficiency of the grown crystals is higher than that of KDP sample which indicates the suitability of crystals for application in nonlinear optical devices and optoelectronic devices.

3.5. CONCLUSION

Optically transparent good quality single crystals of pure TGS and TGS- KDP mixed in the molar ratio (9:1), (8:2) and (7:3) were grown by slow evaporation method from the mixtures of aqueous solution at room temperature. Powder XRD, FTIR and EDAX analysis confirm the fact that the KDP has gone into the lattice sites of the TGS crystals. The presence of various functional groups was confirmed by FTIR spectrum. The UV-Vis-NIR transmission spectra show a wide transparency window without any absorption. TGS - KDP mixed crystals generate optical second harmonic frequency of an Nd:YAG laser. It is found that the SHG efficiency of the TGS:KDP (9:1) mixed crystal is 1.0125 times greater than KDP, TGS:KDP (8:2) is 0.975 times greater than KDP and TGS:KDP (7:3) is 1.112 times

greater than KDP. The relative SHG efficiency of the grown crystals is higher than that of KDP sample which indicates the suitability of crystals for application in nonlinear optical devices and optoelectronic devices. This study will be helpful to grow high quality TGS crystals with good piezoeletric, laser damage threshold and SHG efficiency for various applications.

3.6 References

1. M.Banan, R.B.Lal, A.K.Batra, Journal of materials science, 27 (1992), 2291-2297.
2. K. Meera, R. Muralidharan, P. Santhanaraghavan, R.Gopalakrishnan, P. Ramasamy, Journal of Crystal Growth, 226 (2001), 303–312.
3. G. Arunmozhi*, S. Lanceros-Me´ndez, E. de Matos Gomes, Materials Letters 54 (2002), 29–336.
4. A. J. Jeyaprakash Manoharan, N. Joseph John, V. Revathi, K. V. Rajendran and P.M. Andavan, Indian Journal of Scienceand Technology, Vol. 4 No. 6 (June 2011).
5. P.Manoharan and N.Neelakanda Pillai, *Available online at* www.scholarsresearchlibrary.com, Scholars Research Library Archives of Applied Science Research, 2013, 5 (1):93-97
6. R. Renugadevi et al./ Elixir Crystal Growth 55A (2013) 13033-13035.
7. K. Balasubramanian , P. Selvarajan and E. Kumar, Indian Journal of Science and Technology, Vol. 3 No. 1 (2010).
8. Ferdousi Akhtar, Jiban Podder,Journal of Crystallization Process and Technology, 2011,1, 55-62.
9. S.K.Kurtz, T.T.Perry, J.Appl. Phys.., 39,3798. (1968).
10. Kavya.H, Bhayashree.M and Dr.R.AnandaKumari, Growth and characterization of ADP single crystals doped with Alkali and Alkaline metal ions, ICC-2015, International conference on condensed matter & Applied physics.

CHAPTER-4

Growth and Characterization of Triglycine Sulphate (TGS) Crystal mixed with Ammonium Dihydrogen Orthophosphate (ADP)

4.1 INTRODUCTION

Triglycine Sulphate crystals have technological importance for room-temperature infrared detectors, earth exploration, radiation monitoring and astronomical telescopes. TGS undergoes a second-order ferroelectric phase transition at Curie temperature T_C = 49^0C, ferroelectric and pyroelectric materials are polar and possess a spontaneous Polarization. However, this polarity can be reversed through the application of an electric field with ferroelectric materials [1-4]. They are similar to ferromagnetic materials in that they exhibit hysteresis loops. This material has found application in the fabrication and development of infrared detectors due to its high pyroelectric coefficient (p), reasonably low dielectric constant and best figure-of-merit. TGS crystals have been focused in various aspects such as growth rate, structural modification, pyroelectric, mechanical, optical and ferroelectric properties. Also the crystals are of particular interest for the photo induced nonlinear optical effects. TGS has a tendency to depole, which can be prevented by suitably mixing optically active molecules in the glycine site of TGS.

Triglycine sulphate (TGS) is a ferroelectric crystal. The ferroelectric crystals find important applications in optoelectronics, photonics and used in the fabrication of high sensitivity infrared detectors at room temperature. TGS was synthesized by taking the AR grade Glycine (CH_2NH_2COOH) and concentrated sulphuric acid (H_2SO_4) in the molar ratio 3:1 respectively. The synthesized pure TGS is mixed with Ammonium dihydrogen Orthophosphate (ADP) in the molar ratio (9:1), (8:2) and (7:3) and the crystals were grown from aqueous solution by slow evaporation method at room temperature. The chemical composition of the grown crystals is confirmed by Energy Dispersive X-ray Analysis (EDAX). The solubility of grown crystals is determined using water as a solvent. The solubility curve shows that the TGS-ADP mixed crystal has higher solubility than the pure TGS. The grown crystals were crushed to a uniform fine powder and subjected to XRD analysis. Appearance of sharp peaks confirms the good crystalline nature. Using Scherer's equation particle size has been calculated. The Second harmonic generation efficiency is determined by Kurtz powder technique. The KDP crystal is used as a reference material, it is found that the relative SHG conversion efficiency of the grown crystals is greater than KDP

sample which indicates the suitability of crystals for various applications. Optical transmission spectra are recorded for the crystals in the wavelength region 200 to 1100 nm using Perkin-Elmer Lambda 35 UV-Vis spectrophotometer. The electronic band transitions is studied from the plot of $(\alpha h\nu)^2$ versus photon energy (hv) and the band gap energy has been calculated. The functional groups have been identified by Fourier Transform Infrared spectroscopy (FTIR). The experimental results evidence the suitability of the grown crystals for optoelectronic applications.

This chapter describes the Solubility, crystal growth, structural, Optical, and SHG efficiency of Triglycine sulphate (TGS) - Ammonium dihydrogen Orthophosphate (ADP) mixed in the molar ratio 9:1, 8:2 and 7:3 grown by slow evaporation method. The effects of mixing ADP crystals on the quality and performance of the crystals are analyzed. The results of the TGS-ADP mixed crystals are compared with the pure TGS crystals.

4.2 EXPERIMENTAL

4.2.1 SYNTHESIS

Triglycine sulfate (TGS) was synthesized by taking glycine and sulfuric acid in the molar ratio 3:1.

$$3(NH_2CH_2COOH) + H_2SO_4 \longrightarrow (NH_2CH_2COOH)_3.H_2SO_4 .$$

The required amount of sulfuric acid was diluted with triple distilled water. Then the calculated amount of glycine was added and dissolved in dilute H_2SO_4. The solution was heated until the salt crystallized. Extreme care was taken during crystallization to avoid the oxidation of glycine.

4.2.2 CRYSTAL GROWTH

The synthesized pure TGS is mixed with AR Grade Ammonium dihydrogen Orthophosphate (ADP) in the molar ratio (9:1), (8:2) and (7:3) separately in the triple distilled water with continuous stirring of 3-4 hours using magnetic stirrer. The completely dissolved solution was filtered using micro filter. The solution was allowed to evaporate at room temperature. Triple distilled water was used as the solvent.

Optically good quality large-size single crystals were obtained in a period of 30 days. All the grown crystals were found to be very stable and transparent. The grown crystals are shown in the figure 1- 4.

FIGURE 1. Photograph of as grown Pure TGS Single crystals

FIGURE 2. Photograph of as grown TGS mixed ADP (9:1) Single crystals

FIGURE 3. Photograph of as grown TGS mixed ADP (8:2) Single crystals

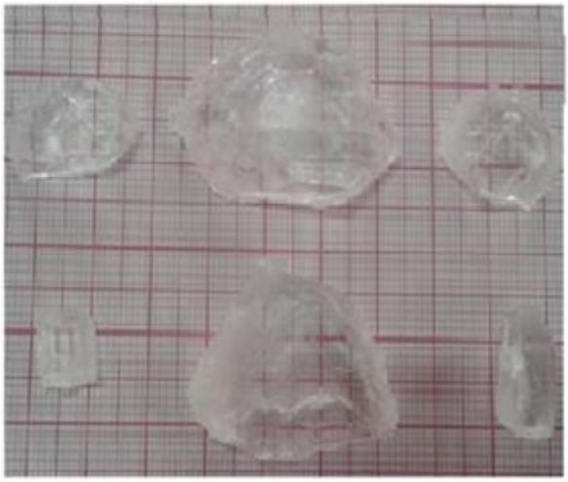

FIGURE 4. Photograph of as grown TGS mixed ADP (7:3) Single crystals

4.3. RESULTS AND DISCUSSION

4.3.1 Energy Dispersive X-ray Analysis (EDAX)

In order to confirm the presence of ADP in pure TGS crystals, the sample of grown crystals were subjected to Energy Dispersive X-ray Analysis. Figures 5a-5c shows the EDAX data of TGS:ADP mixed crystals. From the EDAX and XRAD data, it is confirmed that the ADP has gone into the lattice of the TGS crystals.

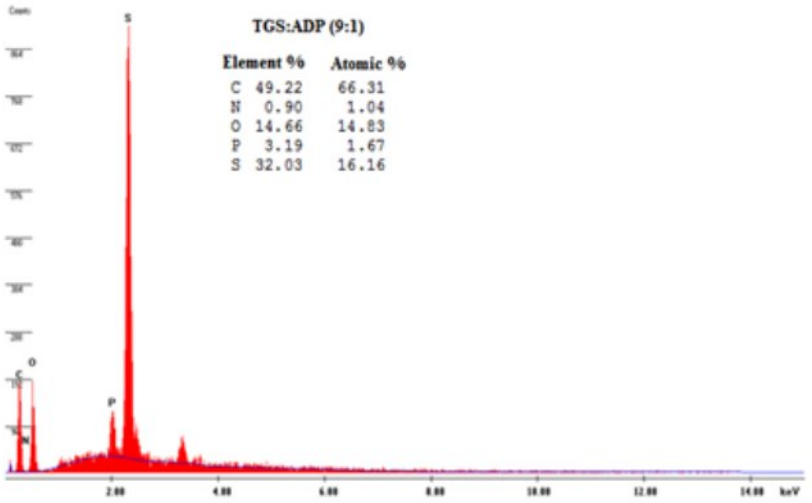

FIGURE 5a. EDAX Spectra of TGS:ADP (9:1) grown crystal

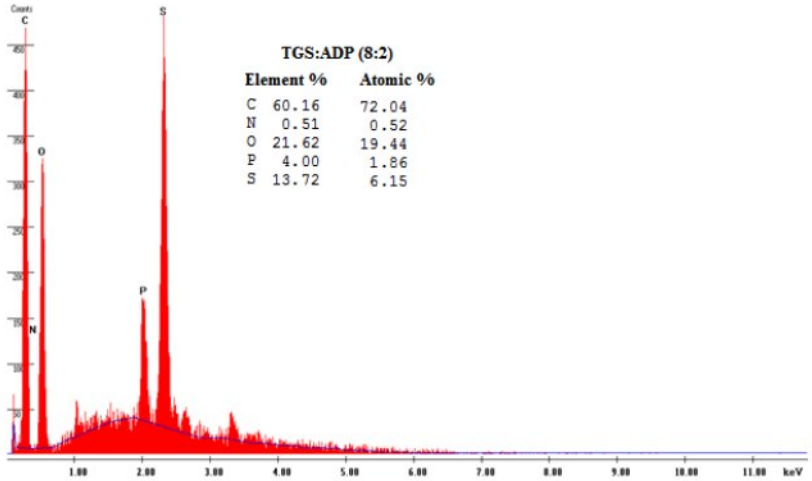

FIGURE 5b. EDAX Spectra of TGS:ADP (8:2) grown crystal

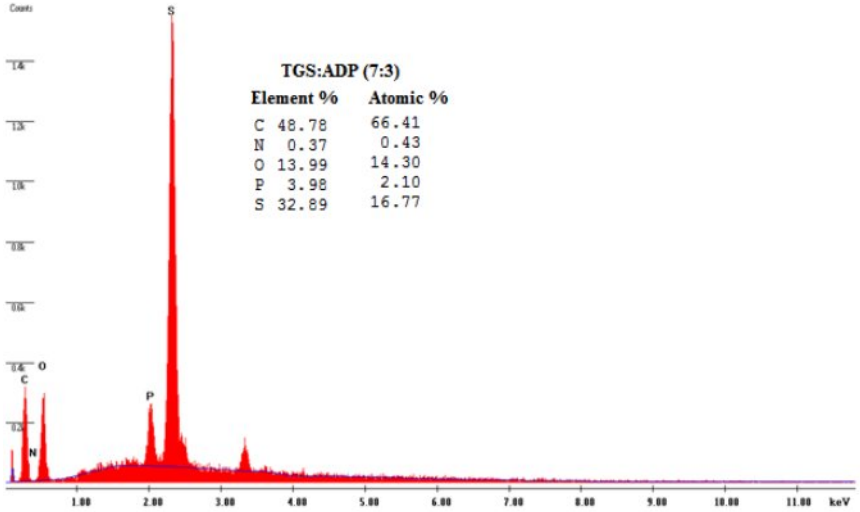

FIGURE 5c. EDAX Spectra of TGS:ADP (7:3) grown crystal

4.3.2 Determination of Solubility

The Solubility studies were carried out in a constant temperature water bath (CTB). The solution was stirred continuously for 6 hours to achieve stabilization using an immersible magnetic stirrer. Solubility was determined by gravimetric analysis for different temperatures (30–50^0 C). The solubility curve of pure TGS, pure ADP, TGS mixed ADP is shown in Figure.6. It is observed from the solubility curve that the solubility of TGS mixed ADP increases with increase in the molar weight of ADP and with respect to pure TGS and pure ADP and has positive temperature co-efficient.

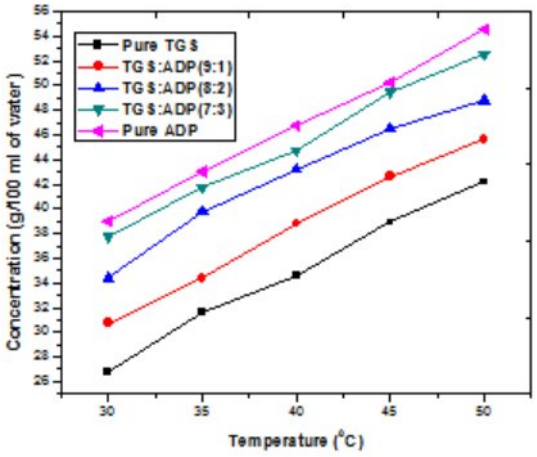

FIGURE 6. Solubility Curve of the grown crystals

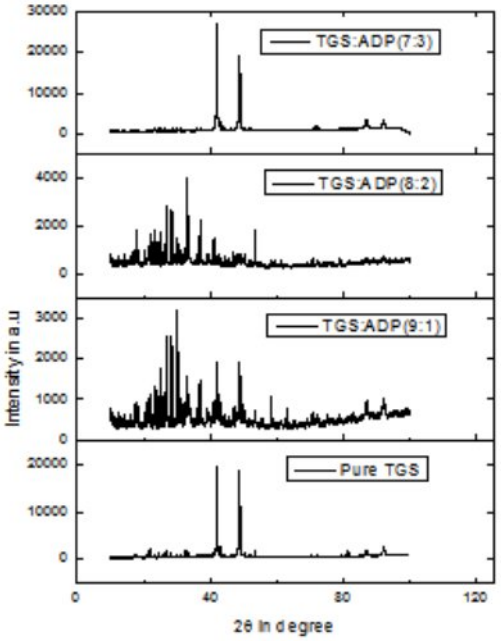

FIGURE 7. Powder X-ray diffraction patterns of grown crystals

4.3.3 XRD Analysis

Good quality grown crystals were crushed to a uniform fine powder and subjected to XRD analysis using XrdwinPD 4-dectris computer based diffractometer with a characteristic Cu Kα (1.540598) radiations from 10^0 to 100^0 at a scan rate of 10^0/min. Appearance of sharp peaks confirms the good crystallinity of the grown samples. The observed values are in good agreement with the reported values [5-6]. The XRD spectra of pure TGS and ADP mixed TGS crystals are shown in Figure 7. Using Scherer's equation (D-S) particle size has been calculated and is given in the Table 1.

TABLE 1. Particle Size Calculated Scherer's (D-S) equation.

Table 2. SHG Signal and SHG efficiency of by

Sample (Crystals)	Average Particle Size (nm)
Pure TGS	26.784
TGS:ADP (9:1)	32.052
TGS:ADP (8:2)	38.145
TGS:ADP (7:3)	15.091

Details of the sample	SHG Signal	SHG Efficiency w.r.t KDP	SHG Efficiency w.r.t TGS
Pure TGS	98mV	1.225	1
TGS:ADP (9:1)	99mV	1.237	1.010
TGS:ADP (8:2)	63mV	0.787	0.642
TGS:ADP (7:3)	72mV	0.9	0.734

4.3.4 Optical transmission studies

Crystal plates of pure TGS and ADP mixed TGS crystals were cut and polished without any coating for optical measurements. The dimensions of the crystals were 10x10x5mm^3. Optical transmission spectra were recorded for the crystals in the wavelength region 200 - 1100 nm using Perkin-Elmer Lambda 35 UV-Vis spectrometer. The recorded UV-Vis spectrum is shown in the Figure 8.

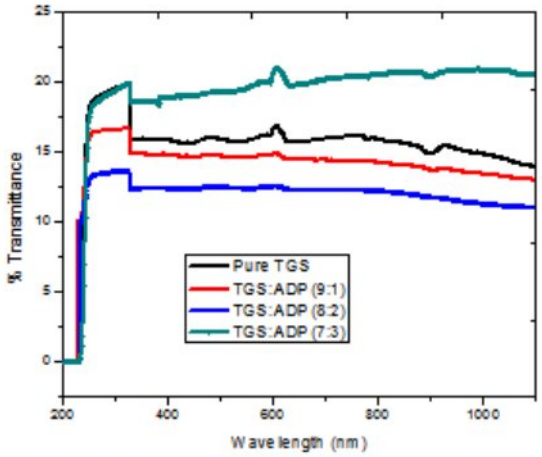

FIGURE 8. UV-Vis transmittance spectra of grown crystals

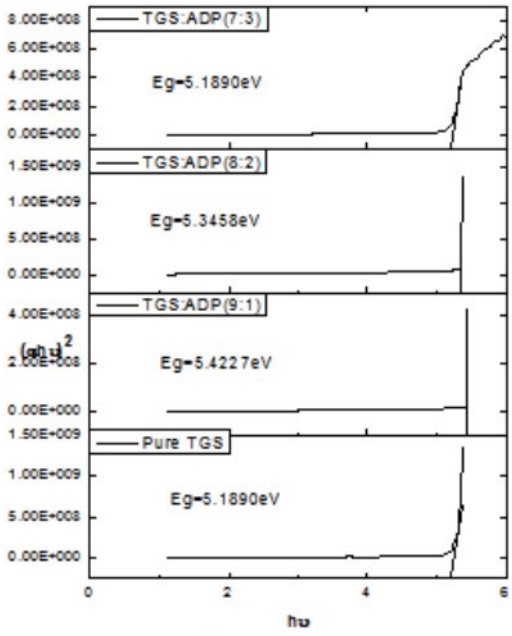

FIGURE 9. $(\alpha h\upsilon)^2$ versus photon energy hv of the grown crystals

Good optical transmittance and lower cut off wavelength are very essential properties for nonlinear optical (NLO) crystals [7]. It is observed from the figure that the Pure TGS shows 19% of transmittance, TGS- ADP (9:1) shows 17% and TGS -ADP (7:3) shows 21% of transmittance. The large transmission in the entire visible region enables it to be a good material for electro-optic and NLO applications. The above results indicate that the addition of ADP to pure TGS increased the transmittance. The plot of $(\alpha h\upsilon)^2$ versus photon energy hv

as shown in Figure 9. The wide optical band gap of TGS:ADP mixed crystals is found to be 5.4227eV, 5.3458eV and 5.1890eV for the molar ratio (9:1), (8:2) and (7:3) respectively suggests its suitability for optoelectronics applications.

4.3.5 FTIR Spectroscopy

The Fourier transform infrared (FTIR) spectra for the powder samples of the grown crystals was recorded in the frequency region 400 - 4000 cm^{-1} using Perkin Elmer spectrometer. The FTIR spectra of pure TGS and TGS-ADP mixed crystals are shown in Figures 10-13.

The mid IR spectrum of TGS shows a broad envelope between 1800 and 2800cm^{-1}. It includes the OH stretch of hydrogen bonded carboxyl groups, the asymmetric stretching mode of NH_3^+ at 3135.386cm^{-1} and CH_2 stretching modes just below 3000 cm^{-1}. The broadening that extends between 2800 and 2200cm^{-1} includes overlapping of bands due to the stretching modes of hydrogen bonded NH^{3+} overtones and combination bands. The C=0 stretch of carbonyl groups display its characteristic peak at 1701.972 cm^{-1}. The CH_2 bending modes of glycine are located at 1374.381cm^{-1} and1423.164cm^{-1}. The NH_3^+ displays its characteristic bending modes at 1423.164, 1491.936 and 1529.171cm^{-1}. The intense and sharp peaks position between 900 and 1000cm^{-1} are assigned to stretching modes of carboxyl and sulphate ions. The peaks due to NH_3^+ oscillation are seen at 895.083, 862.292 and 674.687cm^{-1}. Table 3. shows the vibrational frequencies corresponding to the band assignments of pure TGS and TGS:ADP mixed crystals. The following vibrational assignments showed the hydrogen bonding extends throughout the TGS mixed ADP molecules. These hydrogen bonding results in the modification of stretching frequencies of O-H group of TGS and the carboxyl group of ADP molecules [8]. This confirms the presence of ADP in the pure TGS crystal.

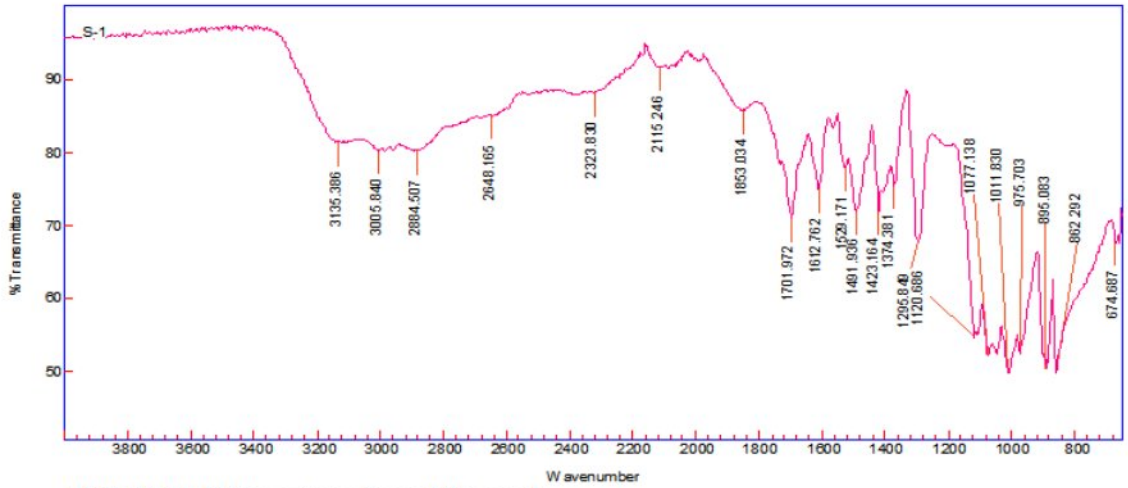

FIGURE 10. FTIR spectrum of pure TGS crystal

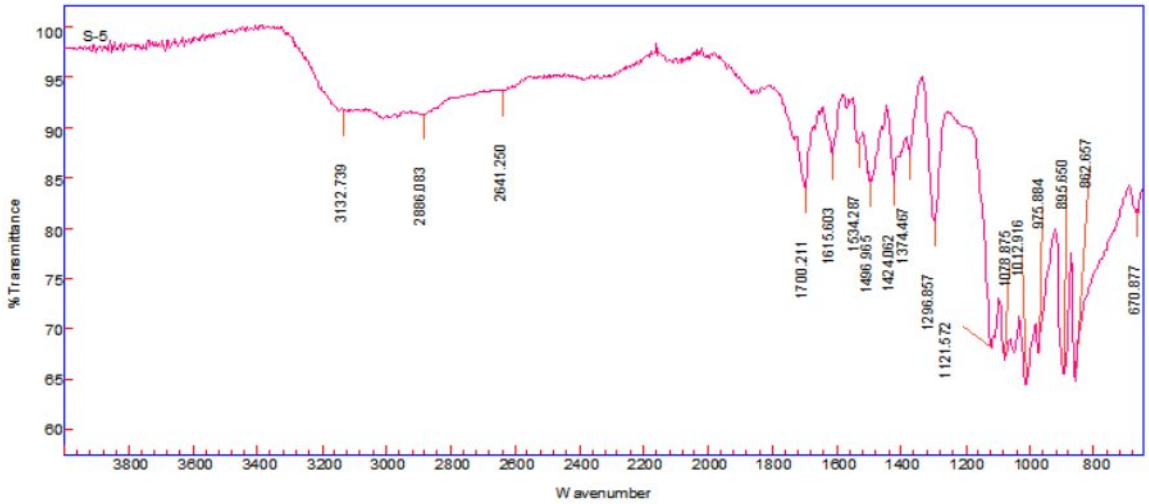

FIGURE 11. FTIR spectrum of the TGS:ADP (9:1) crystal

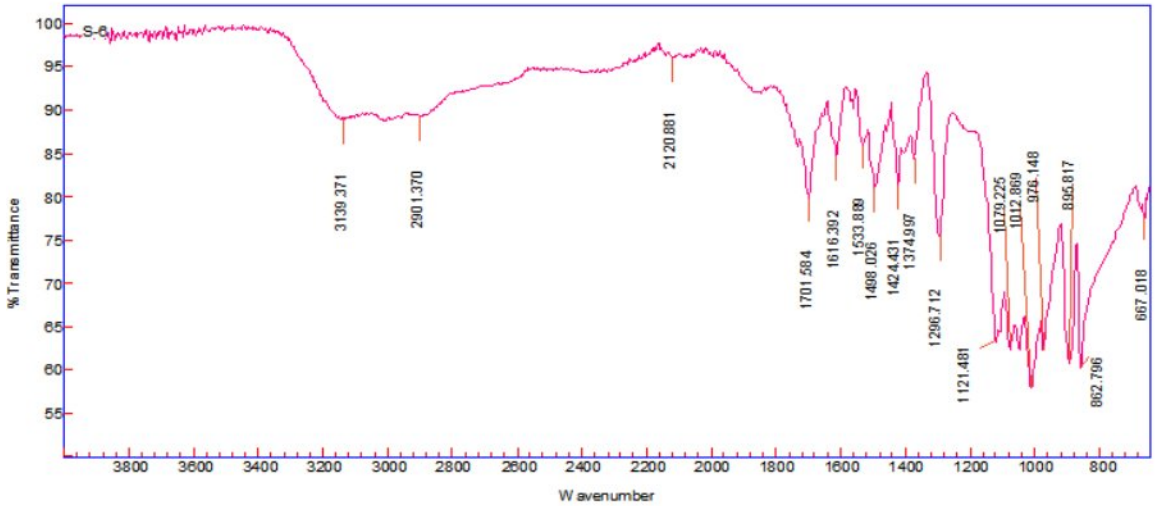

FIGURE 12. FTIR spectrum of the TGS:ADP (8:2) crystal

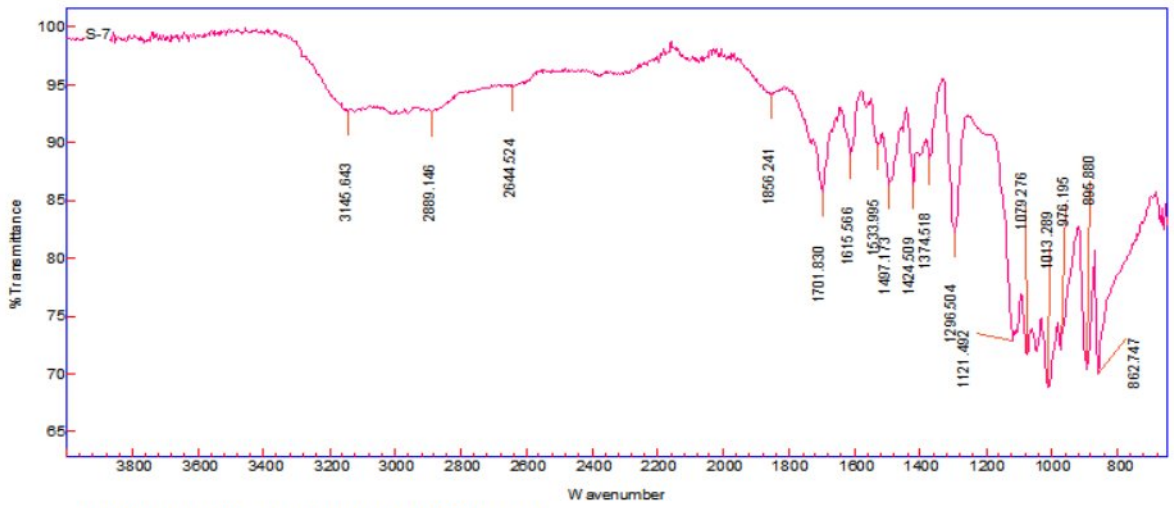

FIGURE 13. FTIR spectrum of TGS:ADP (7:3) crystal

Table 3. Vibrational frequencies for Pure TGS and TGS mixed ADP crystals

Pure TGS	TGS:ADP (9:1)	TGS:ADP (8:2)	TGS:ADP (7:3)	Assignments
3135.386	3132.739	3139.371	3145.643	O-H stretching, H-bonded
3005.840	--	--	--	O-H stretching
2884.507	2886.083	2901.370	2889.146	O-H stretching
2648.165	2641.250	--	2644.524	Intermolecular H-bonded OH streching
2323.830	--		--	C-H stretching
2115.246	--	2120.881	--	O-H Stretching
1853.034	--	--	1856.241	P-O-H symmetric stretching
1701.972	1700.221	1701.584	1701.830	O-P-OH symmetric stretching
1423.164	1424.062	1424.431	1424.509	O-H stretching
1374.381	1374.457	1374.997	1374.518	CH_2 bending, P=O symmetric stretching
1011.830	1012.830	1012.869	1013.289	P-O-H symmetric stretching
975.703	975.884	976.148	976.195	O=P-OH bending
895.083	895.650	895.817	896.880	HO-P-OH bending
862.292	862.657	862.796	862.747	P-OH deformation/K-O stretching
674.687	670.877	667.018	--	PO_4 stretching

4.3.6 Second Harmonic generation Studies (SHG)

The Second harmonic generation efficiency was determined by Kurtz powder technique [9]. Laser beam coming from the source has very high energy. Its intensity is reduced by using glass plates and Neutral density (ND) filter which reduces the intensity and it allows only 1064nm wavelength to incident on the sample taken in a microcapillary tube. Output from the sample is passed through the monochromator which is intensified by photomultiplier tube and finally the signal is observed and read on the Oscilloscope. A Q-switched Nd:YAG laser beam of wavelength 1064nm and 8ns pulse width with an input rate of 10Hz was used to test the NLO property of the sample. The second harmonic signal of 532nm green light was collected by a photomultiplier tube [10]. The optical signal incident on the PMT was converted into voltage output at the cathode ray oscilloscope.

The grown crystals were crushed into fine powder and tightly packed in a microcapillary tube. It was mounted in the path of Nd-YAG laser beam of energy 5mJ/pulse. The KDP crystal was used as a reference material. The transmitted beam voltage for pure KDP was 80mV, for the pure TGS crystal 98mV, 99mV for TGS-ADP (9:1). 63mV for TGS-ADP (8:2) and 72mV for TGS-ADP (7:3) sample. It is found that the SHG efficiency of the TGS-ADP (9:1) mixed crystal is 1.237 times greater than KDP, TGS-ADP (8:2) is 0.787 times greater than KDP and TGS-ADP (7:3) is 0.9 times greater than KDP. The measured values are given in Table 2. The relative SHG efficiency of the grown crystals is higher than that of KDP sample which indicates the suitability of crystals for application in nonlinear optical devices and optoelectronic devices.

4.4. CONCLUSION

Optically transparent good quality single crystals of pure TGS and TGS-ADP mixed in the molar ratio (9:1), (8:2) and (7:3) were grown by slow evaporation method from the mixtures of aqueous solution at room temperature. Powder XRD, FTIR and EDAX analysis confirm the fact that the ADP has gone into the lattice sites of the TGS crystals. The presence of various functional groups was confirmed by FTIR spectrum. The UV-Vis-NIR transmission spectra show a wide transparency window without any absorption. TGS-ADP mixed crystals generate optical second harmonic frequency of an Nd:YAG laser. It is found that the SHG efficiency of the TGS-ADP (9:1) mixed crystal is 1.237 times greater than KDP, TGS-ADP (8:2) is 0.787 times greater than KDP and TGS-ADP (7:3) is 0.9 times greater than KDP. The relative SHG efficiency of the grown crystals is higher than that of

KDP sample which indicates the suitability of crystals for application in nonlinear optical devices and optoelectronic devices. This study will be helpful to grow high quality TGS crystals with good piezoeletric, laser damage threshold and SHG efficiency for various applications.

4.5 REFERENCES

[1] M.Banan, R.B.Lal, A.K.Batra, Journal of materials science, 27 (1992), 2291-2297.

[2] K. Meera, R. Muralidharan, P. Santhanaraghavan, R.Gopalakrishnan, P. Ramasamy, Journal of Crystal Growth, 226 (2001), 303–312.

[3] G. Arunmozhi*, S. Lanceros-Me´ndez, E. de Matos Gomes, Materials Letters 54 (2002) 29 –336.

[4] A. J. Jeyaprakash Manoharan, N. Joseph John, V. Revathi, K. V. Rajendran and P.M. Andavan, Indian Journal of Scienceand Technology, Vol. 4 No. 6 (June 2011).

[5] Farhana Khanum, Jiban Podder, Journal of Crystallization Process and Technology, 1, (2011) 49 - 54.

[6] R. Renugadevi et al./ Elixir Crystal Growth 55A (2013) 13033-13035.

[7] K. Balasubramanian , P. Selvarajan and E. Kumar, Indian Journal of Science and Technology, Vol. 3 No. 1 (2010).

[8] Ferdousi Akhtar, Jiban Podder,Journal of Crystallization Process and Technology, 2011,1, 55-62.

[9] S.K.Kurtz, T.T.Perry, J.Appl. Phys.., 39,3798. (1968).

[10] Kavya.H, Bhayashree.M and Dr.R.AnandaKumari, Growth and characterization of ADP single crystals doped with Alkali and Alkaline metal ions, ICC-2015, International conference on condensed matter & Applied physics.

CHAPTER 5

SUMMARY AND FUTURE PLANS

5.1 SUMMARY OF THE WORK DONE

The growth of organic and inorganic single crystals play a vital role in nonlinear optical (NLO) applications. Growth of high quality crystals with fewer defects is important for the semiconducting industry, material engineering industries etc. There is an increasing demand for highly efficient ferro electric and nonlinear optical materials day by day. Amino acids doped with Triglycinesulphate (TGS) exhibit ferro electric properties and have been investigated in the recent decades. Since glycine is amphoteric in nature, it reacts chemically either as an acid or a base with other compounds to produce large number of possible glycine compounds.

In the present work pure TGS was synthesized by taking the AR grade Glycine (CH_2NH_2COOH) and concentrated sulphuric acid (H_2SO_4) in the molar ratio 3:1 respectively. The synthesized pure TGS is mixed with Potassium dihydrogen Orthophosphate (KDP) and also TGS is mixed with Ammonium dihydrogen Orthophosphate (ADP) in the molar ratio (9:1), (8:2) and (7:3) and the crystals were grown from aqueous solution by slow evaporation method at room temperature. The chemical composition of the grown crystals is confirmed by Energy Dispersive X-ray Analysis (EDAX). The solubility of grown crystals is determined using water as a solvent. The solubility curve shows that the TGS-KDP , TGS-ADP mixed crystal has higher solubility than the pure TGS. The grown crystals were crushed to a uniform fine powder and subjected to XRD analysis. Appearance of sharp peaks confirms the good crystalline nature. Using Scherer's equation particle size has been calculated. The Second harmonic generation efficiency is determined by Kurtz powder technique. The KDP crystal is used as a reference material, it is found that the relative SHG conversion efficiency of the grown crystals is greater than KDP sample which indicates the suitability of crystals for various applications. Optical transmission spectra are recorded for the crystals in the wavelength region 200 to 1100 nm using Perkin-Elmer Lambda 35 UV-Vis spectrophotometer. The electronic band transitions is studied from the plot of $(\alpha hv)^2$ versus photon energy (hv) and the band gap energy has been calculated. The functional groups have been identified by Fourier Transform Infrared spectroscopy (FTIR).

5.2 SUGGESTIONS FOR FUTURE RESEARCH

The results of the present investigations allow ample scope for further investigations in these single crystals as outlined below.

1. It is possible to grow bulk sized unidirectional TGS-KDP and TGS-ADP mixed single crystals with improved optical quality by carefully adopting SANKARANARAYANAN-RAMASAMY method.
2. High resolution X-ray diffraction studies can be carried out to identify the interstitial defects present in the crystals.
3. The growth mechanism of the crystal can be investigated further using the etching pattern of the grown crystals.
4. TG/DTA and DSC analysis can be carried out to analyze the thermal stability of the grown crystals.
5. Thermo mechanical analysis (TMA) can be carried out in future to evaluate the coefficients of thermal expansions (linear and bulk expansion coefficient) to find the thermal stress produced on the crystal.
6. The grown crystals can be fabricated as pyro electric sensors.